Universiteit Leiden
The Netherlands

Semisynthetic glycopeptide antibiotics

Groesen, E. van

Citation

Groesen, E. van. (2022, October 12). *Semisynthetic glycopeptide antibiotics*. Retrieved from https://hdl.handle.net/1887/3480199

Version:	Publisher's Version
License:	Licence agreement concerning inclusion of doctoral thesis in the Institutional Repository of the University of Leiden
Downloaded from:	https://hdl.handle.net/1887/3480199

Note: To cite this publication please use the final published version (if applicable).

Chapter 5 |

Vancomycin-trihydroxamate sideromycins – a Trojan-horse approach

5.1 Introduction

Antimicrobial resistance (AMR) poses a major threat to human health. In 2019, 4.95 million deaths were estimated to be associated with AMR, including 1.27 million deaths directly attributable to AMR infections.[1] The leading cause of nosocomial infections are the so-called ESKAPE pathogens (*E. faecium, S. aureus, K. pneumoniae, A. baumannii, P. aeruginosa,* and *Enterobacter* species), most of which are multi-drug resistant and are becoming increasingly difficult to treat with clinically approved antibiotics.[2,3] Among the ESKAPE pathogens, it is exclusively the Gram-negative species that are indicated as "critical" according to the World Health Organization's priority pathogens list, underscoring the importance of developing novel anti-Gram-negative strategies.[4] One approach to combatting Gram-negative bacterial infections is by potentiating existing antibiotics, which otherwise only work against Gram-positive strains. This strategy has been applied on a variety of Gram-positive specific antibiotics, such as vancomycin.[5–11]

Vancomycin (**Fig. 1**) is a last-resort glycopeptide antibiotic that has been used to treat serious Gram-positive bacterial infections since the 1950s.[12] It acts as a cell-wall biosynthesis inhibitor by binding to the cell-wall precursor lipid II via a network of five-hydrogen bonds, thereby blocking the crosslinking activity of transglycosylases and transpeptidases to form the polymeric cell wall.[13–17] Whereas the peptidoglycan layer and lipid II are readily accessible in Gram-positive strains, Gram-negative bacteria have an outer membrane (OM) barrier, characterized by an inner leaflet of phospholipids and an outer leaflet containing lipopolysaccharide (LPS, endotoxin),[18] which prevents large, hydrophobic antibiotics like vancomycin from reaching its target site. For vancomycin to reach the periplasm of Gram-negative strains, where lipid II resides, transport across the OM is crucial. Previous reports have demonstrated the potential for vancomycin to target Gram-negative strains if it can pass the OM and Shlaes and coworkers confirmed the binding interaction of vancomycin with Gram-negative lipid II of *E. coli*.[19] Bardoel and colleagues proved the sensitization of MDR *K. pneumoniae* to vancomycin in the presence of serum proteins targeting the OM. Specifically, the membrane attack complex of the human complement system residing in serum can form pores in the OM, allowing for enhanced potency of Gram-positive specific antibiotics against the Gram-negative *K. pneumoniae*.[20] Furthermore, successful potentiation of vancomycin against Gram-negative bacteria has been previously reported either by co-administration of,[21–25] or covalent conjugation to,[5–10] OM disrupting moieties. These previous reports stipulate the possibility for vancomycin to exert antimicrobial activity against Gram-negative bacteria when the OM barrier is breached. Besides strategies relying on OM permeabilization, active transport of vancomycin through the OM by bacterial receptors and transporters has been previously explored. In an early study of this kind Miller and coworkers conjugated vancomycin to an iron chelating siderophore mimetic, to yield a hybrid that

showed enhanced potency towards a hypersensitive strain of *P. aeruginosa* under iron depleted conditions.[11] In more recent efforts, they synthesized bis-catechol- and mixed ligand (bis-catechol-mono-hydroxamate)-teicoplanin conjugates active against MDR *A. baumannii.*[26] In addition, the group of Nolan demonstrated that conjugation of the natural iron sequestering siderophore enterobactin to vancomycin results in a hybrid with enhanced potency against *E. coli* and *P. aeruginosa* strains deficient of native siderophore production.[27]

Siderophores are small molecule metabolites excreted by microorganisms to scavenge iron in the environment, and subsequently solubilize and complex with ferric iron with high affinity.[28–30] These molecules are secreted because iron is an essential bacterial nutrient required for numerous enzymatic reactions involved in fundamental cellular processes in bacterial cells.[30] Over 500 siderophores have been identified to date[31] generally containing one of four main iron coordinating moieties: hydroxamates, catecholates, carboxylates, and phenolates, with mixtures of these moieties also prevalent.[32] The most well-known naturally produced siderophore enterobactin (**Fig. 1**), consists of three catecholate moieties linked in a triserine macrocycle[33] and has unparalleled affinity for iron ($K = 10^{52}\ M^{-1}$).[34,35] In addition to uptake of Fe^{2+} by G-protein like receptors[30,36] and Fe^{3+} uptake via host-iron complexes such as lactoferrin, transferrin, and haem,[30,36–38] siderophores are one of the main sources bacteria use for iron acquisition.[30] During an infection, bacterial and host cells continuously compete for acquisition of the extremely low free iron concentrations (e.g. $<10^{24}$ M in human serum).[39] Host cells use lactoferrin and transferrin to chelate extracellular iron and limit its availability for pathogens, while bacteria compete for the iron by secreting the iron-sequestering siderophores, which scavenge the environment for free ferric iron as well as extract iron from the host's iron–protein complexes.[40–43] In Gram-negative bacteria, after complexation with Fe^{3+}, siderophores are recognized by β-barrel outer membrane proteins facilitating TonB-dependent passage across the OM.[34,44,45] Upon release in the periplasm, translocation to the cytosol is usually facilitated by periplasmic-binding proteins and ATP-dependent membrane transporters.[34,44,45] Once inside the cell, the Fe^{3+}-siderophore complex is reduced or hydrolyzed, releasing the iron.[34] This entire process is regulated by ferric uptake regulator Fur, which in high iron environments complexes with ferrous iron and binds the promotor region of siderophore synthesis and regulatory activator genes, thereby repressing their transcription. Under low iron bioavailability, Fur dissociates and siderophore transcription and uptake is promoted.[28,46–48] Siderophores are not only used for harvesting iron in the host-cell microenvironment, but microorganisms also exploit the iron sequestering properties of siderophores in competition against other microorganisms, for example by excretion of antibiotic-conjugated siderophores called sideromycins.[49]

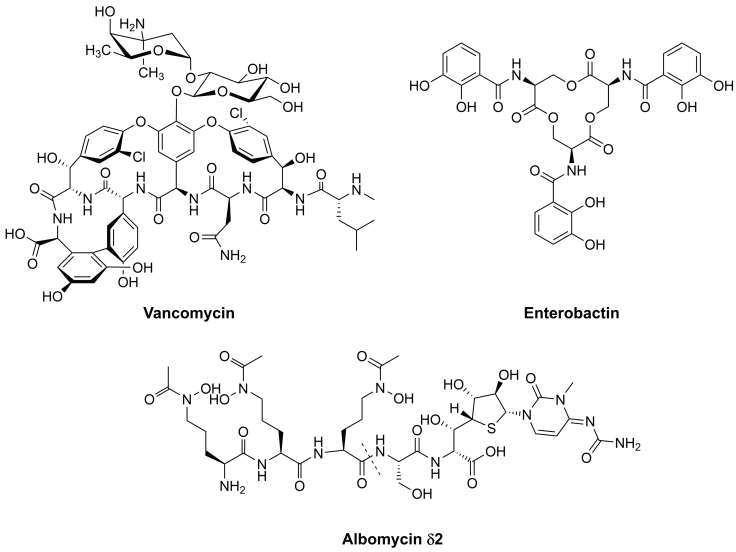

Fig. 1. Structures of vancomycin, enterobactin, and albomycin δ2. Albomycin intracellular peptidase N cleavage site indicated with dashed line (--).

Sideromycins are siderophores that are covalently linked to an antibacterial compound. Using a Trojan-Horse approach, sideromycins are actively transported across the OM to facilitate entry of the antibiotic into the bacterial cell. A few natural sideromycins have been discovered, of which albomycin (**Fig. 1**), discovered in 1947 and produced by *Streptomyces*, is among the best characterized.[49–52] Gause pioneered studies into the structure and activity of albomycin, discovering its iron-dependent mechanism.[53] However, it was not until the 1980s that Benz and coworkers fully elucidated the chemical structure of albomycin.[54] The tri-δ-N-hydroxy-δ-N-acetyl-L-ornithine siderophore of albomycin has structural similarities to ferrichrome and is linked via a L-serine bridge to a thioribosyl pyrimidine antibiotic.[54] Albomycin is transported across the OM by the TonB-dependent FhuA transporter[55–60] and is subsequently transported through the periplasm by FhuD[61,62] towards inner membrane-associated protein FhuB. IM transport is energized by ATPase FhuC, which resides on the cytosolic side of FhuB.[57,63–65] After transport to the cytosol, the antibiotic moiety is cleaved of by peptidase N,[66,67] allowing it to exert its action. Albomycins have potent antibacterial activity against both Gram-negative and Gram-positive pathogens,[53,68,69] and were historically used to treat bacterial infections in patients in the former Soviet Union.[53]

Natural sideromycins have also inspired the design of semisynthetic sideromycins, of which the first was reported as early as 1977 by Zahner and coworkers.[70] Over the years much research has been directed towards designing synthetic sideromycins,[11,33,71–80] a topic that has been extensively reviewed.[31,75,79] Notably, while

synthetic siderophores provide access to structural diversity, when pursuing synthetic sideromycins it appears that natural siderophores offer the most effective iron binding moieties, of which catecholate and hydroxamate units are most commonly explored.[75] For linker moieties, cleavability is considered crucial for antibiotics with cytoplasmic targets, but not for antibiotics with periplasmic targets.[75,81] The conjugation of siderophores to various antibiotic moieties has been reported previously, of which β-lactam antibiotics are most widely explored.[75] The most successful such example is that of cefiderocol (brand name Fetroja), a cephalosporin-catechol sideromycin,[33] which as of 2020 is the first sideromycin approved by the FDA for clinical use against various Gram-negative ESKAPE pathogens.[82] In addition to β-lactam sideromycins, many other siderophore-antibiotic conjugates have been reported, including those linking an iron sequestering agent to anti-Gram-positive antibiotics[75] such as daptomycin,[71,72,80] linezolid,[74,83] erythromycin,[84] and vancomycin.[11,27]

Given previous studies showing that conjugation of siderophores to anti-Gram-positive drugs, including vancomycin, can lead to improved antimicrobial activity against Gram-negative strains.[11,27,71,72,80] we hypothesized that linking vancomycin to the naturally occurring tri-δ-N-hydroxy-δ-N-acetyl-L-ornithine siderophore of albomycin, might allow for transport across the OM barrier, subsequently sensitizing Gram-negative strains to the action of vancomycin. Notably, the most successful semisynthetic siderophore-conjugates reported to date incorporate anti-Gram-positive drugs that have periplasmic targets, such as daptomycin, amino-penicillins and vancomycin.[11,27,71,72,80] Our interest in vancomycin was further spurred by previous reports from our group and others demonstrating the enhanced antibacterial effect of vancomycin-conjugates capable of disrupting the Gram-negative OM.[5,6] In designing our semisynthetic sideromycins, the albomycin trihydroxamate motif was selected as the siderophore given that hexadentate moieties are widely considered to be the most effective in generating synthetic sideromycins.[79,85] Here, we report the synthesis of a novel class of vancomycin-siderophore conjugates, the semisynthetic vancomycin-trihydroxamate sideromycins. The antibacterial activity of these compounds was evaluated against a panel of bacterial strains, including siderophore biosynthesis and transport deletion strains. In addition, the iron-chelating activity and *in vitro* toxicity of these compounds was investigated.

5.2 Results and Discussion

5.2.1 Development of vancomycin-trihydroxamate sideromycins

As a strategy for the preparation of the vancomycin-trihydroxamate sideromycin conjugates **1** and **2 (Fig. 2**) we elected for a convenient "click chemistry" based approach wherein complementary azide and alkyne containing precursors can be linked by means

of the well-established copper-catalyzed azide-alkyne cycloaddition (CuAAC) reaction.[86–88] In pursuit of these conjugates, we incorporated the alkyne handle into the vancomycin structure, while the azide moiety was installed on the trihydroxamate siderophore unit. Given that lipid II, the cell wall precursor target of vancomycin, can reside both in the periplasm and on the cytosolic side of the IM, we also chose to incorporate the peptidase N cleavage site in the peptide-based linker bridging the antibiotic with the siderophore.

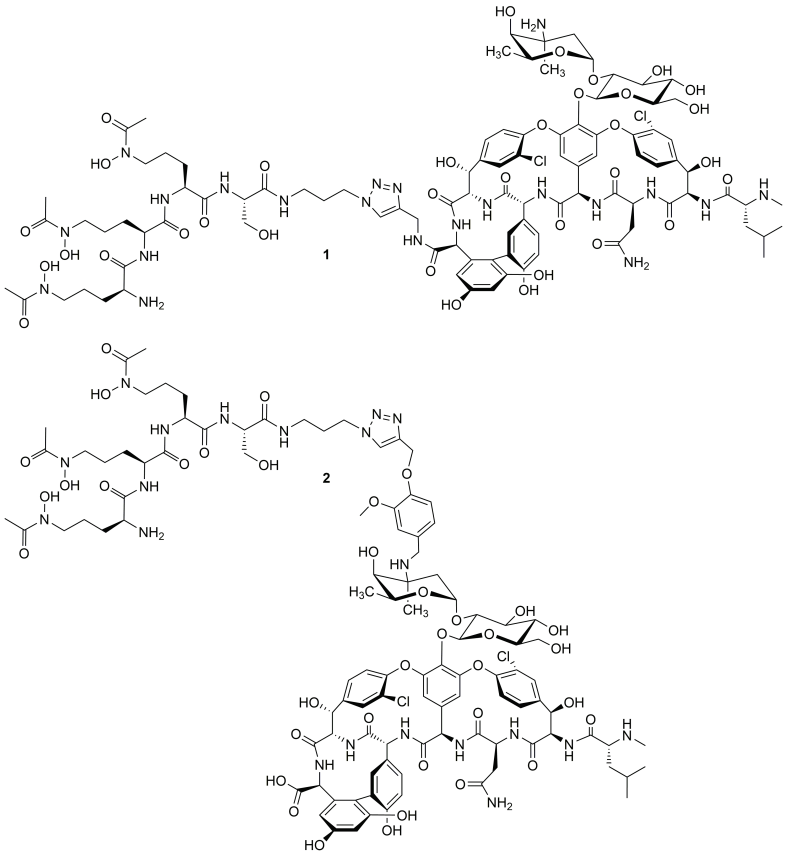

Fig. 2. Vancomycin-trihydroxamate sideromycins 1 and 2.

To obtain the alkyne-modified vancomycin precursors, we followed procedures previously reported by Sharpless and coworkers, who employed the CuAAC reaction to prepare a variety of vancomycin dimers.[88] The alkyne handle was thereby installed at either the vancomycin C-terminus or the vancosamine moiety. Both sites have been widely modified in semisynthetic vancomycin analogues previously described in the literature[89] and were therefore not expected to alter binding of the vancomycin core to lipid II.[5] As previously described in **Chapter 4**, for the preparation of C-terminally alkyne

modified vancomycin, propargyl amine was coupled to vancomycin using HBTU/DIPEA to yield **Int-1**. Introduction of the alkyne moiety at the vancosamine unit was in turn achieved via reductive amination using an alkyne-substituted benzaldehyde building block derived from vanillin to give **Int-2** (see **Scheme S1** and **S2** for details).

For the azide-containing siderophore precursor, we envisioned installing the azide handle at the C-terminal side of the peptidase N cleavage site found in albomycin. To this end we prepared the appropriately modified L-serine building block **5** as indicated in **Scheme 1**. The synthesis commenced with the preparation of azidopropylamine linker **3** following literature protocols.[90] Subsequently, **3** was coupled with Boc-L-Ser(tBu)-OH using HATU/DIPEA to generate **4**, followed by removal of the Boc and *tert*-butyl protected groups by treatment with TFA to yield **5**. This building block was subsequently used in the preparation of the siderophore azide **12** as shown in **Scheme 2**. The preparation of **12** first required the synthesis of the iron chelating motif of albomycin, tri-δ-N-hydroxy-δ-N-acetyl-L-ornithine. The synthesis of this siderophore has been described by the groups of Benz[91,92] and Miller[78,93,94], and more recently by He and coworkers,[52] which is the synthetic procedure we followed. As shown in **Scheme 2**, the synthesis begins with the oxidation of the chain amine of Boc-L-ornithine *tert*-butyl ester with benzoyl peroxide, followed by acylation with AcCl to yield a the fully protected hydroxamate **6**. Next, the acid sensitive *tert*-butyl-carbonate and *tert*-butyl groups were removed using TFA to yield **7**, after which the free amine group was reprotected as the Fmoc carbamate to obtain **8**. Iterative dipeptide (**9**) and subsequent tripeptide (**10**) synthesis was achieved using active amide-mediated conditions as described by Katritzky,[95–98] minimizing the risk of epimerization.[52] Condensation of the tripeptide tri-δ-N-hydroxy-δ-N-acetyl-L-ornithine **10** to the azide-containing serine **5** using HATU/DIPEA yielded tetrapeptide **11**. Simultaneous removal of the Fmoc and benzoyl groups using K_2CO_3 then afforded the C-terminal azide-modified albomycin siderophore **12**.

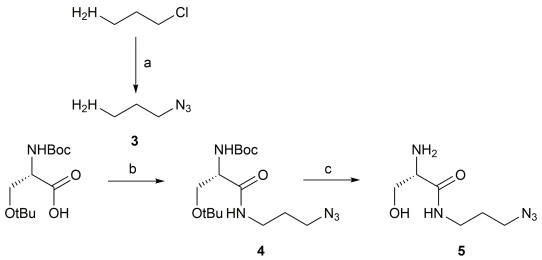

Scheme 1. Synthesis of azide-containing L-serine linker 5. a) NaN_3, H_2O, 80 °C; b) **3**, HATU, DIPEA, DMF, 0 °C then RT; c) TFA, H_2O, RT.

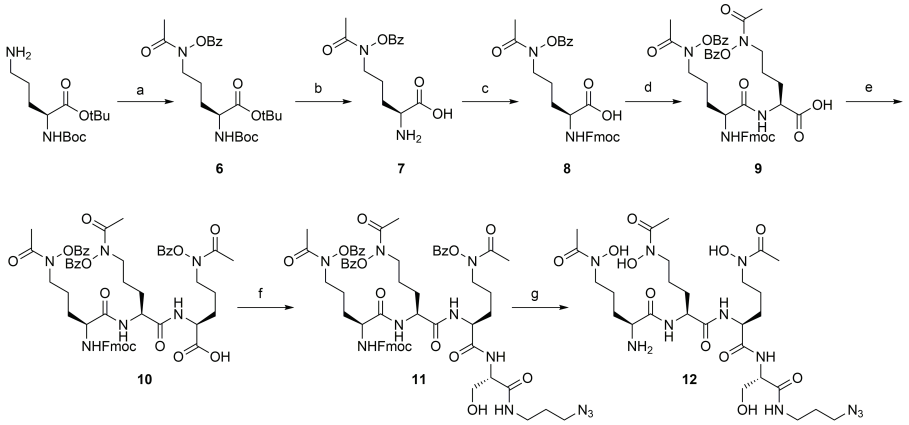

Scheme 2. Synthesis of azide-modified albomycin siderophore 12. a) BPO, CH_2Cl_2, $NaHCO_3$ buffer pH 10, then AcCl, RT; b) TFA, H_2O, RT; c) Fmoc-OSu, NEt_3, DMF, -15 °C; d) i. BtH, $SOCl_2$, THF, -15 °C then RT. ii. **7**, NEt_3, CH_3CN/H_2O, -15 °C then RT; e) i. BtH, $SOCl_2$, THF, -15 °C then RT. ii. **7**, NEt_3, CH_3CN/H_2O, -15 °C then RT; f) **5**, HATU, DIPEA, DMF, 0 °C; g) K_2CO_3, CH_3CN/H_2O, RT.

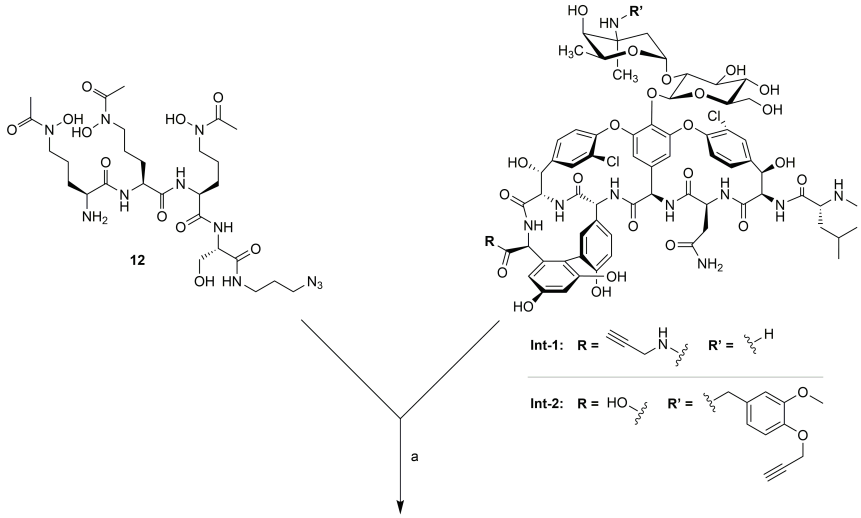

Conjugates **1** and **2** (see Figure 2)

Scheme 3. Synthesis of vancomycin-trihydroxamate sideromycins 1-2. a) $CuSO_4$, THPTA, sodium ascorbate, H_2O, RT.

With the required azide-containing siderophore (**12**) and alkyne-containing vancomycin (**Int-1** and **Int-2**) building blocks in hand, conjugation was accomplished by means of triazole formation (**Scheme 3**). The click reaction was performed using copper catalysis,[86–88] with $CuSO_4$, Cu^I-stabilizing ligand tris(3-hydroxypropyltriazolylmethyl)amine (THPTA)[99,100], and sodium ascorbate, conditions previously used by Gotsbacher and Codd to achieve CuAAC on desferrioxamine

siderophores.[100] In all cases the ligation reactions proceeded smoothly to generate the final vancomycin-trihydroxamate sideromycins **1** and **2** in 89-94% yield after HPLC purification.

5.2.2 Assessment of *in vitro* antibacterial activity

The antibacterial activities of the vancomycin-trihydroxamate sideromycins **1** and **2**, as well as the alkyne and azide building blocks (**Int-1**, **Int-2**, compound **12**), were assessed against a panel of Gram-negative pathogens, including strains of *E.coli*, *K. pneumoniae*, *A. baumannii,* and *P. aeruginosa*. Since siderophore transport across the OM by TonB-dependent transporters is highly specific for the type of siderophore structure,[101] all tested bacterial strains were selected based on the presence of the *fhuA* gene in their genome, as FhuA is the β-barrel outer membrane protein responsible for the transport of ferrichrome-like structures such as tri-δ-N-hydroxy-δ-N-acetyl-L-ornithine and albomycin[55]. The presence of this transporter was hypothesized to be crucial in order for the vancomycin-trihydroxamate sideromycins to exhibit activity, as OM passage of vancomycin is essential for it to reach the periplasm, where lipid II resides. Antibacterial activity was determined in two different media: Iron-depleted cation-adjusted Mueller Hinton Broth (CAMHB), prepared according to CLSI procedure, and iron-repleted CAMHB, which was prepared from iron-depleted CAMHB supplemented with 0.2 mg/L Fe^{3+}. Iron-depleted CAMHB, containing ≤0.02 mg/L iron, is commonly used to test the antimicrobial activity of sideromycins as it: 1) induces ferric iron transporters in bacteria,[28,46,47,102–104] 2) replicates the iron concentrations in the human tissue and fluids,[104] and 3) has previously been shown to have predictive value in mirroring the *in vivo* efficacy of the clinically approved sideromycin cefiderocol.[105] Broth microdilution assays revealed compounds **1** and **2**, as well as the alkyne and azide building blocks (**12**, **Int-1**, **Int-2**), to be inactive against a panel of Gram-negative strains, regardless of the iron concentration in the media (**Table 1**, see **Table S1** for μM concentrations).

Upon visual inspection of the microplates, it was found that wells containing *P. aeruginosa* ATCC27853 were much brighter in color (yellow-green) in iron-depleted conditions compared to iron-repleted conditions (**Fig. 3**). Since the naturally produced siderophore of *Pneudomonas*, pyoverdine,[106] is yellow-green,[107] this observation led us to hypothesize that the vancomycin-trihydroxamates cannot compete with the natural siderophores produced by the Gram-negative bacterial strains tested, an effect not uncommon for synthetic sideromycins.[79,108,109] Successful iron scavenging by pyoverdine has shown to trigger increased siderophore production in a positive feedback loop,[48] which can explain the color intensity of the growth media. To confirm this hypothesis, the antibacterial activity of the vancomycin-trihydroxamate sideromycins against a siderophore-deficient strain was next assessed. For this study *E. coli* BW25113 was

selected as a model strain for several reasons: 1) this strain is a commonly used lab strain which has the *fhuABCD* genes[110] that translate to the proteins facilitating trihydroxamate uptake,[55,61,62,110] 2) a library, known as the Keio collection, with single-gene deletions of all non-essential genes of this strain is readily available[111], and 3) *E. coli* BW25113 produces only one natural siderophore, enterobactin, thus deletion of a single gene is sufficient to create a non-siderophore-producing strain.

Table 1. *In vitro* activity of the vancomycin-trihydroxamate sideromycins against a panel of Gram-negative strains.

	MIC (µg/mL)					
	E. coli			***K. pneumonia***	***A. baumannii***	***P. aeruginosa***
	ATCC 25992	**ATCC 35218**	**BW 25113**	**ATCC 13883**	**BAA-747**	**ATCC 27853**
Iron-repleted CAMHB						
Vancomycin	>128	>128	256	>128	>128	>128
1	>128	>128	>256	>128	>128	>128
2	>128	>128	>256	>128	>128	>128
12	>128	>128	>256	>128	>128	>128
Int-1	128	64	64	>128	>128	>128
Int-2	>128	>128	>256	>128	>128	>128
Iron-depleted CAMHB						
Vancomycin	>128	>128	128	>128	>128	>128
1	>128	>128	>256	>128	>128	>128
2	>128	>128	>256	>128	>128	>128
12	>128	>128	>256	>128	>128	>128
Int-1	64	64	64	>128	>128	>128
Int-2	>128	>128	>256	>128	>128	>128

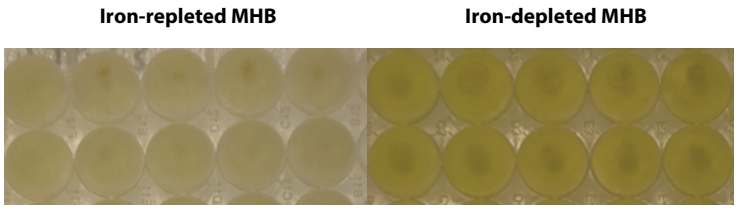

Fig. 3. *P. aeruginosa* ATCC 27853 growth under iron-repleted (left) and iron-depleted (right) conditions.

The vancomycin-trihydroxamate sideromycins were tested against an *entA* deletion strain of *E. coli* BW25113 (**Table 2**, see **Table S2** for µM concentrations). EntA oxidizes dihydro-2,3-dihydroxybenzoate to dihydro-2,3-dihydroxybenzoate dehydrogenase,[112,113] a key step for enterobactin biosynthesis. In iron-depleting conditions, the antibacterial activity of both compound **1** and **2** was enhanced ≥32-fold to 8 µg/mL against this enterobactin-deficient strain compared to the wild-type enterobactin-producing *E. coli* (MIC ≥256 µg/mL) and ≥16-fold compared to vancomycin. Notably, supplementation with exogenous enterobactin antagonized the

activity of our vancomycin-trihydroxamate sideromycins, causing the MIC values to be elevated to the same level as observed when tested against the wild-type *E. coli* BW25113 strain (MIC ≥256 µg/mL). These observations indicate that the increased potency against *ΔentA* is due to the absence of enterobactin production. This increased potency of the vancomycin-trihydroxamate sideromycins suggests effective transport through the OM, allowing the vancomycin moiety to reach its target site and exert its action. These results are in line with previously reported potencies of vancomycin against Gram-negative strains upon OM disruption[5,6]. Alternatively, the sideromycins could deprive the *E. coli* of iron, which also can result in lower MIC values.[27] Similar results were obtained for iron-repleted conditions, with no more than 2-fold differences compared to iron-depleted media, which could be attributed to induction of ferric iron transporters in iron-depleted conditions.[102–104]

Table 2. *In vitro* activity of the vancomycin-trihydroxamate sideromycins against *E. coli* BW25113 and *Δent* with and without exogenous enterobactin supplementation.

	MIC (µg/mL)		
	***E. coli* BW25113**		
	WT	***ΔentA***	***ΔentA* + 8 µg/mL enterobactin**
Iron-repleted CAMHB			
Vancomycin	256	128	128
1	>256	16	>256
2	>256	16	>256
12	>256	>256	>256
Int-1	64	64	64
Int-2	>256	>256	>256
Iron-depleted CAMHB			
Vancomycin	128	128	128
1	>256	8	>256
2	>256	8	>256
12	>256	>256	>256
Int-1	64	64	64
Int-2	>256	>256	>256

The antibacterial activities of the vancomycin-trihydroxamate sideromycins were further assessed against other mutants with disrupted enterobactin production or transport including the well characterized: *ΔentC* (enterobactin biosynthesis), *ΔtolC* (enterobactin secretion), and *ΔfepABD* (enterobactin uptake) deletion strains. The antibacterial activities measured against these strains are summarized in **Table 3** (see **Table S3** for µM concentrations). Deletion of *entC*, which isomerizes chorismate to isochrismate in the enterobactin biosynthesis,[112,113] results in similar enhanced potency of the vancomycin-trihydroxamate sideromycins **1** and **2** (≥16-fold) as for the *ΔentA* mutant, further confirming the sideromycins to be effective in *E. coli* deprived of enterobactin biosynthesis. The activity of **1** and **2** was also enhanced against the enterobactin export deletion (*ΔtolC*) strain with an increase in potency of ≥16-fold. TolC is responsible for

enterobactin secretion and mutations have previously shown to cause accumulation of periplasmic enterobactin in *E. coli*.[114] An explanation for this observation could be that the inability of the *ΔtolC* mutant to secrete enterobactin may force the bacteria to acquire iron via other siderophores making it more likely to take up vancomycin-trihydroxamate sideromycins **1** and **2**. Alternatively, it could also be that the enhanced antibacterial activity of **1** and **2** towards the *ΔentC* and *ΔtolC* mutants is due to their chelation of all available iron, thereby depriving the cells of iron, rather than successful OM passage.[27] The activity of **1** and **2** was also tested against enterobactin import deletions *ΔfepA*, *ΔfepB*, and *ΔfepD*, which are required for siderophore import across the OM and IM.[115–118] Although the potency of **1** was slightly enhanced (≥2-8-fold), no enhancement was found for **2**. Furthermore, slight enhancements of vancomycin activity (2-fold) could point to the inherently more sensitive nature of these deletion strains, as defective enterobactin-dependent iron uptake was previously reported to result in increased sensitivity to a variety of compounds.[119–121]

Table 3. *In vitro* activity of the vancomycin-trihydroxamate sideromycins against *E. coli* BW25113 and enterobactin biosynthesis, export and import deletion strains.

	MIC (µg/mL)						
	E. coli BW25113						
	WT	***ΔentA***	***ΔentC***	***ΔtolC***	***ΔfepA***	***ΔfepB***	***ΔfepD***
		biosynthesis		**export**	**import**		
Iron-repleted CAMHB							
Vancomycin	256	128	128	256	64	128	128
1	>256	16	32	32	128	64	64
2	>256	16	32	32	>256	256	>256
12	>256	>256	>256	>256	>256	>256	>256
Int-1	64	64	64	64	128	64	64
Int-2	>256	>256	>256	>256	>256	>256	>256
Iron-depleted CAMHB							
Vancomycin	128	128	128	128	64	64	64
1	>256	8	16	16	128	32	64
2	>256	8	16	16	>256	256	>256
12	>256	>256	>256	>256	>256	>256	>256
Int-1	64	64	64	64	64	64	64
Int-2	>256	>256	>256	>256	>256	>256	>256

Overall, loss of enterobactin biosynthesis and export appears to most significantly enhance the activity of vancomycin-trihydroxamate sideromycins **1** and **2** (≥16-32-fold). Deficiency in enterobactin import also resulted in improved activity for **1**, although not as prominently as for the biosynthesis or export deletion strains. Given that the import-deletion strains (unlike biosynthesis and export deficient strains) are still able to produce and secrete enterobactin, the reduced potency of **1** and **2** against the import-deletion strains could also be reflective of a stronger chelation efficiency for enterobactin vs. that of the trihydroxamate-moiety in **1** and **2**.[34,35] Resistance to synthetic sideromycins

due to presence of native siderophores with stronger iron binding ability is not uncommon, and is generally paired with reduced sideromycin assimilation and upregulation of native siderophore transporters.[79,108,109]

The demonstrated potency of **1** and **2** against enterobactin biosynthesis deletion strains points to either the sideromycin's ability cross the OM to access their target lipid II, or their ability to deprive the bacterial cells of iron. To establish if OM disruption would further potentiate sideromycins **1** and **2**, their synergistic effects with the known OM-disruptor polymyxin B nonapeptide (PMBN)[122] was assessed (**Table 4**, see **Table S4** for µM concentrations). Disruption of the OM by covalent linkage to OM-targeting peptides[5,6] or exogenous supplementation of OM disruptors[21–25] has been shown to enhance vancomycin potency to Gram-negative bacteria. While the activity of compounds **1** and **2**, as well as vancomycin, improved slightly against the WT *E. coli* strain upon addition of exogenous PMBN, no enhancement was observed with the *ΔentA* mutant. This finding indicates that in the absence of enterobactin, the vancomycin-trihydroxamate sideromycins exert antibacterial action without need for OM disruption.

Table 4. *In vitro* activity of the vancomycin-trihydroxamate sideromycins against *E. coli* BW25113 and *ΔentA* in the presence and absence of exogenous outer membrane disruptor PMBN.

	MIC (µg/mL)			
	***E. coli* BW25113**			
	WT	**WT + 8 µg/mL PMBN**	***ΔentA***	***ΔentA* + 8 µg/mL PMBN**
Iron-repleted CAMHB				
Vancomycin	256	64	128	64
1	>256	64	16	16
2	>256	256	16	16
12	>256	>256	>256	>256
Int-1	64	32	64	32
Int-2	>256	128	>256	128
Iron-depleted CAMHB				
Vancomycin	128	64	128	32
1	>256	32	8	8
2	>256	128	8	8
12	>256	>256	>256	>256
Int-1	64	32	64	16
Int-2	>256	128	>256	64

Given that the glycopeptide core of the sideromycins remains intact; we anticipated compounds **1** and **2** to retain anti-Gram-positive activity, similarly to vancomycin. Assessment against a panel of vancomycin-sensitive and -resistant *S. aureus* strains revealed, however, a somewhat reduced antibacterial activity for **1** and **2** compared to vancomycin (8-16-fold), although activity was not completely compromised (**Table 5**, see **Table S5** for µM concentrations). These findings suggest that the introduction of the

albomycin trihydroxymate siderophore unit interferes with lipid II target engagement by the glycopeptide moiety.

Table 5. *In vitro* activity of the vancomycin-trihydroxamate sideromycins against Gram-positive *S. aureus* strains.

	MIC (µg/mL)			
	S. aureus			
	ATCC 29213	**MRSA USA300**	**NRS384**	**BR-VRSA**
Iron-repleted CAMHB				
Vancomycin	1	1	1	>128
1	8	8	8	>128
2	16	16	16	>128
12	>128	>128	>128	>128
Int-1	0.5	1	0.5	>128
Int-2	1	2	1	>128
Iron-depleted CAMHB				
Vancomycin	1	1	1	>128
1	4	8	8	>128
2	8	16	16	>128
12	>128	>128	>128	>128
Int-1	1	1	0.5	>128
Int-2	1	2	1	>128

5.2.3 Iron sequestering by the sideromycins

The studies with the deletion strains described above revealed that disruption of enterobactin biosynthesis and export, but not uptake, improves vancomycin-trihydroxamate sideromycin potency. We speculated this difference could be correlated to the competition between naturally secreted enterobactin and the vancomycin-trihydroxamates **1** and **2** for the chelation of ferric iron. As the uptake of sideromycin antibiotics relies on their iron-chelation activity,[42,45] successful sequestration of ferric iron is considered crucial for the antimicrobial activity of **1** and **2**. Enterobactin is, however, one of the strongest chelators for Fe^{3+}, and the presence of significant quantities of this native siderophore in the growth media could diminish the potency of **1** and **2** by sequestering all available ferric iron. The chelating activity of the vancomycin-trihydroxamate sideromycins for iron was therefore determined using a chrome azurol S dye (**Fig. 4**). This colorimetric assay is commonly used to detect siderophores by monitoring reduction in absorbance at 630 nm (A_{630}) associated with the iron-bound form of the dye.[105,123,124] In this assay, we found EDTA and enterobactin both strongly and rapidly chelate Fe^{3+} (**Fig. 4AB**), while compound **1** and **2** appear to do so in a time-dependent manner: after one hour incubation Fe^{3+} sequestering was minimal, but over the

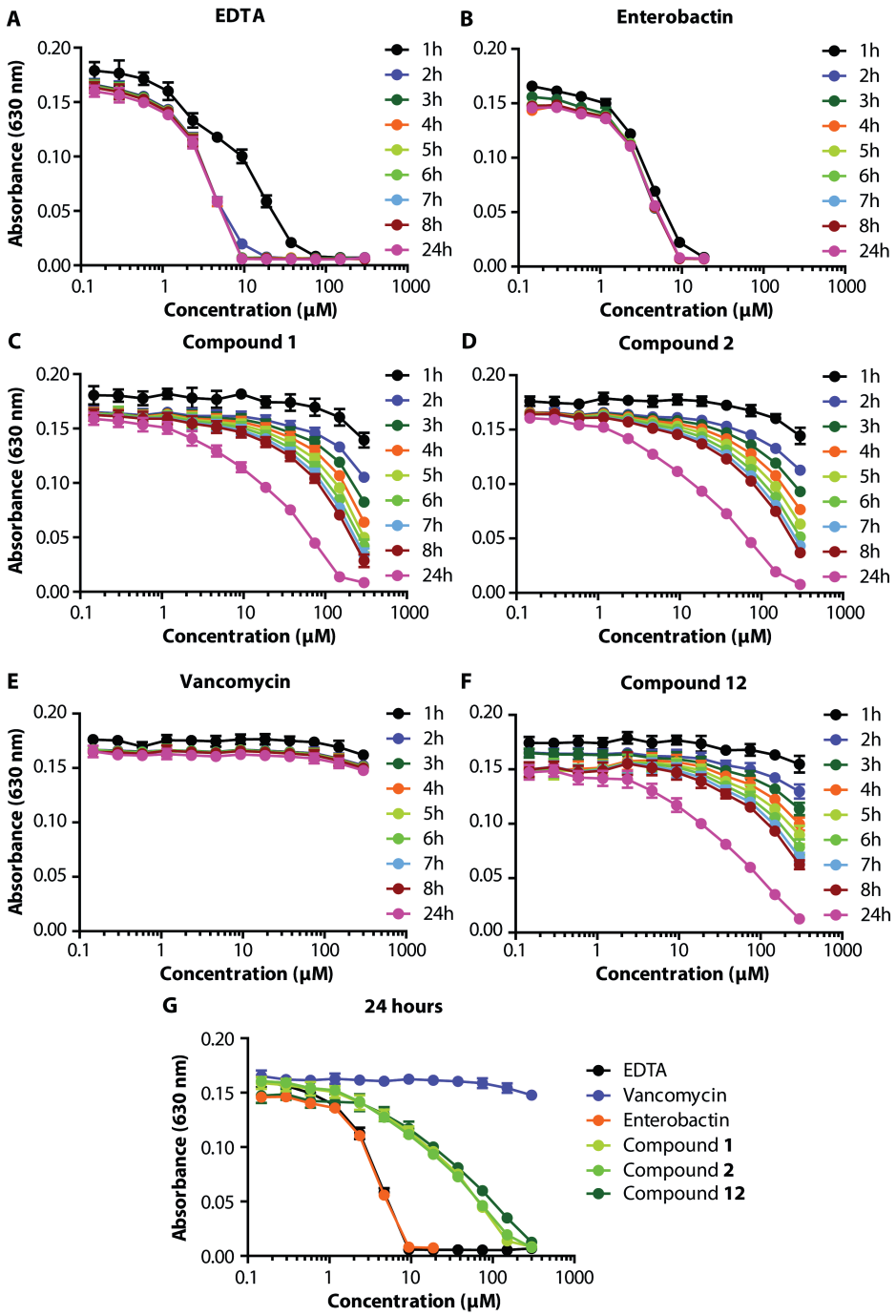

Chelation of ferric iron by different components as detected by decrease in A_{630}.

course of 24 hours clear iron chelation by **1** and **2** did occur, although higher concentrations of both **1** and **2** were required for full iron sequestration relative to **Fig. 4.** enterobactin (**Fig. 4CDF**). The difference in chelating abilities between the vancomycin-trihydroxamates and enterobactin suggest that **1** and **2** cannot outcompete enterobactin's iron chelating abilities, which also provides an explanation for the absence of antibacterial activity for **1** and **2** against siderophore-excreting strains. Moreover, because iron chelation is likely influenced by the protonation state of the trihydroxymate moiety in **1** and **2**, the pKa of the siderophore donors must be taken into consideration when establishing iron complexation efficacy.[34] Hydroxamates have pK_a values ranging from 8-9 whereas the pK_a for catecholates (like enterobactin) ranges from 6.5-8 for dissociation of the first proton.[34] Therefore, the assay conditions (pH 5.6) may not reflect the optimal chelation conditions for the vancomycin-trihydroxamate sideromycins **1** and **2**. In addition, the pH of growth media (pH 7.3) may therefore also not favor iron chelation for trihydroxamate-containing sideromycins. Nonetheless, the iron chelating capacity of enterobactin is unmatched,[34,35] making it impossible for the vancomycin-trihydroxamate sideromycins to outcompete its iron-sequestering abilities. In line with expectations, control experiments with trihydroxamate-azide **12** showed that it has iron chelating properties similar to compound **1** and **2**, whereas vancomycin was unable to chelate ferric iron (**Fig. 4EF**).

5.2.4 Additional *in vitro* cell-based assays

The diminished activity of **1** and **2** against vancomycin-sensitive Gram-positive bacteria was surprising, as the glycopeptide core required for binding to lipid II remained intact. Therefore we assessed whether the sideromycins still act as late-stage cell-wall biosynthesis inhibitors. Upon treatment with cell-wall active antibiotics such as vancomycin and other glycopeptide antibiotics,[125–127] the soluble cell-wall precursor UDP-MurNAc-pentapeptide accumulates in *S. aureus*, an effect that is detectable by HPLC analysis. Treatment of *S. aureus* with compound **1** and **2** also resulted in UDP-MurNAc-pentapeptide accumulation (**Fig. 5**). The extent of the accumulation for bacteria treated with **1** and **2** appears less prominent than vancomycin, which correlates with the diminished *in vitro* activity against Gram-positive strains (although quantitative conclusions cannot be drawn from this assay).

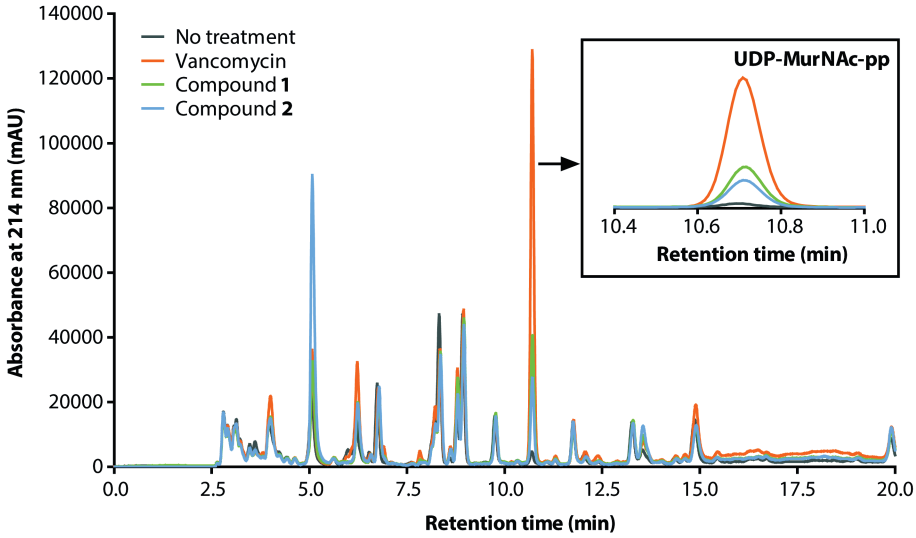

Fig. 5. UDP-MurNAc-pentapeptide accumulation of the vancomycin-trihydroxamate sideromycins.

Preliminary toxicity studies were also performed by assessing the hemolytic potential of compounds **1** and **2** against sheep erythrocytes. Such assays can provides an indication of the general membrane disruptive properties of a compound. These assays revealed no appreciable hemolysis by the vancomycin-trihydroxamate sideromycins **1** and **2** up to the highest concentration tested (256 µg/mL) (**Fig. 6**).

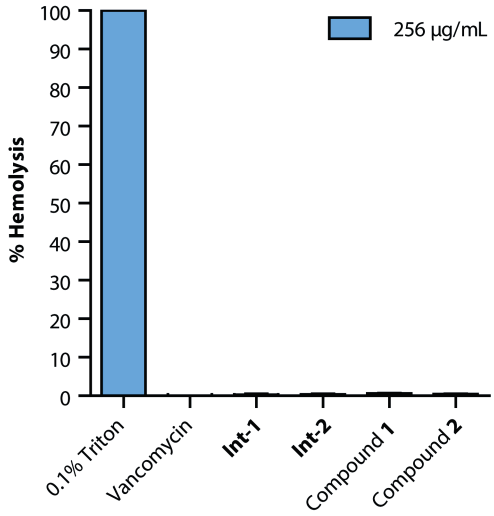

Fig. 6. Hemolytic assessment of the vancomycin-trihydroxamate sideromycins.

5.3 Conclusions

While vancomycin is an important last-resort antibiotic in the clinic against Gram-positive infections, it is ineffective against Gram-negative strains as it cannot cross the OM and access lipid II. Given that vancomycin has affinity for *E. coli* lipid II,[19] circumvention of the OM to potentiate vancomycin against Gram-negative strains has been widely studied.[20,23–25] To this end, vancomycin catecholate siderophore conjugates have been previously explored.[11,27] However, the conjugation of vancomycin to the trihydoyxymate motif, as present in natural sideromycin albomycin, has not been described. In this study we report novel vancomycin-siderophore hybrids, the vancomycin-trihydroxamate sideromycins **1** and **2**. These sideromycins were found to display little-to-no activity against a panel of siderophore producing Gram-negative bacteria. However, against strains deprived of native siderophores, in which genes essential for their biosynthesis (Δ*entAC*) or export (Δ*tolC*) are deleted, **1** and **2** display enhanced potency, an effect reversed upon exogenous enterobactin supplementation. The improved antibacterial activity of **1** and **2** against such mutant strains might be a result of effective transport of the sideromycins across the OM to the target site and/or iron-deprivation of the bacterial strains. Further OM disruption does not contribute to improved antibacterial activities. Future studies to assess effective vancomycin-trihydroxamate transport to the periplasm should be aimed at determining their antibacterial activity against ferrichrome uptake and enterobactin biosynthesis deficient strains (Δ*fhuA*Δ*entA*). Enterobactin import deletions (Δ*fepABD)* cause a less prominent reduction in MIC compared to biosynthesis and export deficient strains, likely due to the difference in chelating efficiency of the sideromycins compared to enterobactin. Reduced binding to ferric iron was further confirmed in a colorimetric assay. Activity against Gram-positive strains was diminished compared to native vancomycin, although late-stage cell wall biosynthesis inhibition was still confirmed. Additionally, the vancomycin-trihydroxamate sideromycins have no hemolytic activity. In summary, covalent linkage of siderophores to vancomycin has the potential enhance the activity of vancomycin against Gram-negative bacteria deprived of endogenous siderophores. Considerations in design of next-generation vancomycin sideromycins should be directed at conjugation of siderophores that circumvent resistance due to the presence of intrinsic siderophores as well as modifications which avoid the attenuation of antibacterial activity now seen against Gram-positive strains.[79]

5.4 Experimental Methods

General methods. All reagents were commercially available, American Chemical Society (ACS) grade or finer and used without further purification unless stated otherwise. For characterization of new compounds, high resolution mass spectrometry (HRMS) was

performed on a Shimadzu Nexera X2 UHPLC system with a Waters Acquity HSS C_{18} column (2.1 × 100 mm, 1.8 µm) at 30 °C and equipped with a diode array detector. At a flow rate of 0.5 mL/min, a solvent system with solvent A, 0.1% formic acid in H_2O, and solvent B, 0.1% formic acid in CH_3CN, was used. Gradient elution was as follows: 95:5 (A/B) for 1 min, 95:5 to 15:85 (A/B) over 6 min, 15:85 to 0:100 (A/B) over 1 min, 0:100 (A/B) for 3 min, then reversion back to 95:5 (A/B) for 3 min. This system was connected to a Shimadzu 9030 QTOF mass spectrometer (ESI ionization) calibrated internally with Agilent's API-TOF reference mass solution kit (5.0 mM purine, 100.0 mM ammonium trifluoroacetate and 2.5 mM hexakis(1*H*,1*H*,3*H*-tetrafluoropropoxy)phosphazine) diluted to achieve a mass count of 10000. LCMS analyses were performed on a Shimadzu LC-20AD system with a Shimadzu Shim-Pack GISS-HP C18 column (3.0 x 150 mm, 3 µm) at 30 °C and equipped with a UV detector monitoring at 214 and 254 nm. The following solvent system, at a flow rate of 0.5 mL/min, was used: solvent A, 0.1 % formic acid in water; solvent B, acetonitrile. This system was connected to a Shimadzu 8040 triple quadrupole mass spectrometer (ESI ionisation). Purity and confirmation of the synthesis of small molecule building blocks, although previously reported in the literature, was assessed with nuclear magnetic resonance (NMR). Spectra were obtained from a Bruker DPX-300, super conducting magnet with a field strength of 7.0 Tesla, equipped with 5 mm BBO, Broadband Observe probe head, high resolution with Z- Gradient, and a 5 mm ^{19}F / ^{1}H dual high-resolution probe. Compounds were purified using preparative high performance liquid chromatography (HPLC) using a BESTA-Technik system with a Dr. Maisch Reprosil Gold 120 C_{18} column (25 × 250 mm, 10 µm) and equipped with a ECOM Flash UV detector monitoring at 214 nm and a flow rate of 12 mL/min. Purity of the final compounds was assessed by integration and confirmed to be >95% unless stated otherwise (see supporting information **Fig. S1**), using analytical reverse phase HPLC (RP-HPLC) using a Shimadzu Prominence-i LC-2030 system with a Dr. Maisch ReproSil Gold 120 C_{18} column (4.6 × 250 mm, 5 µm) at 30 °C and equipped with a UV detector monitoring at 214 nm. At a flow rate of 1 mL/min, a solvent system with solvent A, 0.1% TFA in H_2O/CH_3CN 95:5, and solvent B, 0.1% TFA in H_2O/CH_3CN 5:95, was used. Gradient elution was as follows: 95:5 (A/B) for 2 min, 95:5 to 0:100 (A/B) over 55 min, 0:100 (A/B) for 2 min, then reversion back to 95:5 (A/B) over 1 min, 95:5 (A/B) for 2 min.

*Copper-catalyzed azide-alkyne cycloaddition to synthesize vancomycin-siderophores (**1-2**).* To vancomycin-alkyne **Int-1** or **Int-2** (11-12 µmol, 1 eq) in H_2O (2.5 mL), siderophore-azide **12** (11-12 µmol, 1 eq) was added. $CuSO_4{\cdot}5H_2O$ (1.1 µmol, 0.1 eq), THPTA (2.2 µmol, 0.2 eq), and sodium ascorbate (4.4 µmol, 0.4 eq) in H_2O (2.5 mL) were added to the flask. The reaction was stirred overnight and monitored by LCMS. In case of incomplete conversion, additional $CuSO_4{\cdot}5H_2O$ (0.1 eq), THPTA (0.2 eq), and sodium ascorbate (0.4 eq) in H_2O was added. Upon reaction completion, the mixture was

centrifuged for 5 min at 4500 rpm, after which it was directly purified using the preparative high performance liquid chromatography (HPLC) using a C_{18} column (25 × 250 mm, 10 µm) with UV detection at 214 nm. The following method was used: flow rate = 12 mL/min; solvent A, 0.1% TFA in H_2O/CH_3CN 95:5, and solvent B, 0.1% TFA in H_2O/CH_3CN 5:95. The gradient elution was as follows: 95:5 (A/B) for 5 min, 95:5 to 40:60 (A/B) over 50 min, 40:60 to 0:100 (A/B) for 1 min, 0:100 (A/B) for 2 min, then reversion back to 95:5 (A/B) over 1 min, 95:5 (A/B) for 2 min. Fractions were immediately freeze dried and subsequently analyzed by LCMS. Pure product containing fractions were redissolved, pooled, and lyophilized to yield the vancomyxins as white powders. Yield: 89-94%. **1**: HRMS (ESI): $[M+H]^+$ calculated: 2188.8309, found: 2188.8295. **2**: HRMS (ESI): $[M+H]^+$ calculated: 2325.8674, found: 2325.8675. For purity see **Fig. S1**.

*Synthesis of **3**.* Azide **3** was synthesized according to a previously described procedure.[90] In short, to a solution if 3-chloropropan-1-amine (HCl salt, 38 mmol, 1 eq) in H_2O, NaN_3 (115 mmol, 3 eq) was added and the mixture was stirred overnight at 80 °C. The mixture was basified with aqueous KOH (2M, 49 mL) and extracted with Et_2O three times. The organic layers were combined and dried over $NaSO_4$, filtered and evaporated *in vacuo* to yield **3**, which was used crude in the next reaction.

*Synthesis of **4**.* To a solution of Boc-L-Ser(tBu)-OH (7.7 mmol, 1 eq) in DMF at 0 °C, **3** (8.4 mmol, 1.1 eq), DIPEA (15.3 mmol, 2 eq), and HATU (11.5 mmol, 1.5 eq) were added. The reaction was stirred at RT until completion. The solvent was evaporated and the residue was redissolved in DCM. The organic layer was washed with H_2O and brine, dried over $NaSO_4$, filtered, and evaporated. The product was purified by flash chromatography (2/1 PE/EtOAc). Yield: Quantitative. ^{1}H NMR (300 MHz, $CDCl_3$) δ/ppm 6.67 (s, 1H), 5.38 (s, 1H), 4.10 (s, 1H), 3.76 (dd, J = 8.7, 3.8 Hz, 1H), 3.42 – 3.28 (m, 5H), 1.77 (p, J = 6.7 Hz, 2H), 1.43 (s, 9H), 1.16 (s, 9H).^{13}C NMR (75 MHz, $CDCl_3$) δ/ppm 171.03, 155.61, 80.24, 74.01, 61.92, 54.58, 49.07, 36.87, 28.83, 28.40, 27.53. HRMS (ESI): $[M+H]^+$ calculated: 344.2298, found: 344.2295.

*Synthesis of **5**.* Azide **4** (3.5 mmol, 1 eq) was dissolved in TFA (10 mL) and H_2O (17.9 mmol, 5 eq) and stirred for 12 h at RT. The solvent was evaporated, after which the residue was redissolved in MeOH and evaporated *in vacuo*. This process was repeated three times and the residue was used crude in the next reaction.

*Synthesis of **6**.* Ester **6** was synthesized according to a previously described procedure[52] with minor adjustments. To a solution of BPO (36.9 mmol, 1.2 eq) in DCM (300 mL), Boc-Orn-OtBu (HCl salt, 30.8 mmol, 1 eq) in buffer ($NaHCO_3$ buffer adjusted with NaOH to pH 10.5, 300 mL) was added quickly. The mixture was stirred for 7 h at RT.

Acetyl chloride (30.8 mmol, 1 eq) in DCM (30 mL) was added and the reaction was stirred overnight at RT. The H_2O layer was extracted with DCM three times, after which the organic layers were combined and washed with brine. The DCM layer was dried over $NaSO_4$, filtered and evaporated. The product was purified by flash column chromatography with 3/1 PE/EtOAc. Yield: 83%. HRMS (ESI): $[M+H]^+$ calculated: 451.2444, found: 451.2442.

*Synthesis of **8***. First, carboxylic acid intermediate **7** was synthesized according to a previously described procedure[52] with minor alterations. Ester **6** (24 mmol, 1 eq) was dissolved in TFA (50 mL) and H_2O (120 mmol, 5 eq), and stirred at RT for 12 h. The solvent was evaporated, after which the residue was redissolved in MeOH and evaporated *in vacuo*. This process was repeated three times and the residue was used crude in the next reaction. Then, carboxylic acid **8** was synthesized according to a previously described procedure[52] with minor adjustments. In short, to a solution of crude intermediate **7** (~12.8 mmol, ~1 eq) in DMF (40 mL) at -15 °C, NEt_3 (38.4 mmol, 3 eq) and Fmoc-OSu (15.4 mmol, 1.2 eq) were added. The reaction was stirred at -15°C for 1 h and subsequently acidified to pH 5 with aqueous HCl (1 M). Solvent was removed *in vacuo* and the residue was diluted with EtOAc. The organic layer was washed with aqueous HCl (1 M) and brine, and subsequently dried over $NaSO_4$, filtered and evaporated. The product was purified by flash column chromatography using DCM with 0-5% MeOH gradient. Yield: 35% over two steps. HRMS (ESI): $[M+H]^+$ calculated: 517.1975, found: 517.1971

*Synthesis of **9***. Carboxylic acid **9** was synthesized according to a previously described procedure[52] with minor adjustments. To a solution of 1*H*-benzotriazole (29.1 mmol, 5 eq) in THF (20 mL), thionyl chloride (7.3 mmol, 1.25 eq) was added. The mixture was stirred at RT for 20 min, and subsequently cooled to -15 °C. Compound **8** (5.8 mmol, 1 eq) in THF (10 mL) was added dropwise, and the reaction was stirred at RT for 30 min. The white precipitate was filtered off and the filtrate was concentrated *in vacuo*. The mixture was diluted with EtOAc, and the precipitate was filtered off again and washed with EtOAc. The residue was evaporated to obtain crude active amide, which was added to a solution of carboxylic acid **7** (6.4 mmol, 1.1 eq) with NEt_3 (3.1 eq) in a mixture of CH_3CN/H_2O (20 mL / 8 mL) cooled at -15 °C. The mixture was stirred at RT for 1 h, and the CH_3CN was evaporated. The residue was diluted with EtOAc, and the organic layer was washed with aqueous HCl (0.5 M) and brine. The organic layer was dried with $NaSO_4$ and concentrated *in vacuo*. The product was purified by flash column chromatography with DCM + 1% AcOH → DCM/MeOH 95/5 + 1% AcOH. Yield: 28%. HRMS (ESI): $[M+H]^+$ calculated: 793.3085, found: 793.3084.

*Synthesis of **10***. Carboxylic acid **10** was synthesized according to a previously described procedure[52] with minor adjustments, and as described for **9**. The reaction was carried out

starting from **9** (1.6 mmol, 1 eq) and employed 1*H*-benzotriazole (6 eq) and thionyl chloride (1.5 eq). Yield: 55%. HRMS (ESI): $[M+H]^+$ calculated: 1069.4195, found: 1069.4190

*Synthesis of **11**.* To a solution of carboxylic acid **10** (692 µmol, 1 eq) in DMF (15 mL), azide **5** (761 µmol, 1.1 eq) and HATU (1.0 mmol, 1.5 eq) were added. DIPEA (1.4 mmol, 2 eq) was added dropwise at 0 °C and the reaction was stirred for 3 h at 0 °C. The mixture was acidified to pH 5 with aqueous HCl (1 M) and evaporated *in vacuo*. The mixture was redissolved in EtOAc, and washed with aqueous HCl (0.5 M), saturated aqueous $NaHCO_3$ and brine. The organic layer was dried over $NaSO_4$, filtered and evaporated. The product was purified by flash column chromatography with DCM + 1% AcOH → DCM/MeOH 95/5 + 1% AcOH. Yield: 35%. ^{1}H NMR (300 MHz, $CDCl_3$) δ/ppm 8.12 – 7.97 (m, 6H), 7.71 (d, *J* = 7.4 Hz, 2H), 7.68 – 7.55 (m, 5H), 7.54 – 7.41 (m, 6H), 7.35 (t, *J* = 7.4 Hz, 2H), 7.30 – 7.22 (m, 3H), 7.10 – 7.03 (m, 1H), 6.41 (s, 1H), 4.62 – 4.36 (m, 2H), 4.36 – 4.08 (m, 4H), 4.08 – 3.58 (m, 8H), 3.36 – 3.24 (m, 3H), 2.12 – 1.88 (m, 14H), 1.87 – 1.62 (m, 9H). ^{13}C NMR (75 MHz, $CDCl_3$) δ/ppm 174.7, 173.3, 171.9, 170.6, 164.9, 164.8, 164.6, 157.4, 143.7, 143.6, 141.3, 134.8, 130.1, 129.0, 127.8, 127.2, 126.3, 125.2, 120.0, 67.4, 62.5, 55.9 55.7, 55.7, 54.7, 48.8, 47.6, 47.0, 36.72, 28.5, 27.7, 27.5, 24.45, 24.2, 23.8, 20.4, 20.3. HRMS (ESI): $[M+H]^+$ calculated: 1238.5158, found: 1238.5150. For purity see **Fig. S1**.

*Siderophore-azide **12**.* To a solution of azide **11** (165 µmol, 1 eq) in MeOH, aqueous K_2CO_3 (1 M, 330 µL, 2 eq) was added and the reaction war stirred at RT for 1 h. Additional portions of aqueous K_2CO_3 (1 M, 330 µL, 2 eq) were added and stirred for 1 h until the reaction reached completion. The mixture was acidified to pH 7 with aqueous HCl (1 M). The solvent was evaporated and the solid was washed three times with DCM. The residue was used crude in the next reaction. For biological assessment, a portion was purified using preparative HPLC using a 12 mL/min flow rate. Solvent A was 0.1% TFA in H_2O/CH_3CN 95:5 and solvent B was 0.1% TFA in H_2O/CH_3CN 5:95. Gradient for elution was 0-100% buffer B over 55 min. HRMS (ESI): $[M+H]^+$ calculated: 704.3691, found: 704.3687. For purity see **Fig. S1**.

Table 6. HR-MS analysis

Sample ID	Chemical formula	Calculated M + H	Calculated (M+2H)/2	Measured
1	$C_{96}H_{127}Cl_2N_{21}O_{34}$	2188.8309	1094.9194	2188.8295, 1094.9191
2	$C_{104}H_{134}Cl_2N_{20}O_{37}$	2325.8674	1163.4376	2325.8675, 1163.4365
3	$C_3H_8N_4$	101.0827	51.0453	101.0821
4	$C_{15}H_{29}N_5O_4$	344.2298	172.6188	344.2295
5	$C_6H_{13}N_5O_2$	188.1147	94.5613	188.1144
6	$C_{23}H_{34}N_2O_7$	451.2444	226.1261	451.2442
7	$C_{14}H_{18}N_2O_5$	295.1294	148.0686	295.1290
8	$C_{29}H_{28}N_2O_7$	517.1975	259.1027	517.1971
9	$C_{43}H_{44}N_4O_{11}$	793.3085	397.1582	793.3084
10	$C_{57}H_{60}N_6O_{15}$	1069.4195	535.2137	1069.4190
11	$C_{63}H_{71}N_{11}O_{16}$	1238.5158	619.7618	1238.5150
12	$C_{27}H_{49}N_{11}O_{11}$	704.3691	352.6885	704.3687

Iron-depleted and iron-repleted CAMHB. Iron-depleted CAMHB was made according to CLSI procedures. In short, 100 g Chelex-100 (wet bead size 150-300 µm) was added to 1 L of autoclaved MHB and stirred for 2 h at RT. The media was filter-sterilized using sterile 0.2 µm bottle top filters into an autoclaved empty flask. The pH was adjusted to 7.2-7.4 using aqueous HCl (1 M). The media was filter-sterilized again using sterile 0.2 µm bottle top filters into empty autoclaved flasks. To complete the iron-depleted CAMHB, 0.5 mM $CaCl_2$, 0.5 mM $MgSO_4$ and 10 µM $ZnSO_4$ (from 1 M stocks in H_2O, filter-sterile) were added to the media. For iron-repleted CAMHB, 2.5 µM $FeCl_3$ was added as well.

Broth microdilution assays. From glycerol stocks, bacteria were plated out on blood agar plates overnight at 37 °C. One colony was transferred to growth media and grown at 37 °C at 200 rpm to exponential growth phase as determined by OD_{600} in iron-repleted CAMHB. For VRSA the media was supplemented with 6 µg/mL vancomycin at this stage. For the deletion strains, 25 µg/mL kanamycin was added to the media during this phase. At OD_{600} = 0.5 the bacteria were diluted 100-fold in either iron-repleted or iron-depleted CAMHB and 50 µL was added to a 2-fold serial dilution series of test compound (50 µL) in the same media to reach a total volume of 100 µL per well. The 96-well polypropylene plates were incubated at 37 °C at 600 rpm overnight (18-20 h for Gram-negative strains, 20-24 h for Gram-positive strains) and inspected for visual bacterial growth. Trailing was observed for some strains and taken into account in recording the MIC values as described previously for cefiderocol.[104,128] Synergy experiments were performed in a similar manner as the MIC assay, except 8 µg/mL PMEN or enterobactin final concentration was added to the wells. MICs are reported as the median of triplicates.

Chelating activity with ferric iron. The iron chelation was assessed according to a previously described procedure.[129] In short, 0.75 mL of 1 mM $FeCl_3$ dissolved in 10 mM

HCl was added to 3.75 mL of 2 mM chrome azurol S solution in H_2O. The mixture was added to 3 mL of a 10 mM cetyltrimethylammonium bromide. 42.5 mL of 0.588 M MES pH adjusted with 50% KOH to pH 5.6 was added to the dye (achieving a final MES concentration of 0.5 M). In a clear flat-bottom plate, to a serial dilution of compound (50 µL), 50 µL dye solution was added to all wells except blank well (100 µL H_2O). Absorbance was measured at 630 nm at 1 , 2, 3, 4, 5, 6, 7, 8, and 24 h. Plates were incubated at RT in the dark at 170 rpm between measurements.

UDP-MurNAc-pentapeptide accumulation. From glycerol stocks, *S. aureus* ATCC29213 was cultured on blood agar plates and incubated overnight at 37 °C. A single colony was grown in TSB + 0.002% p80 overnight at 37 °C and diluted 100-fold in fresh media. The bacterial culture was grown at 37 °C (200 rpm) until exponential phase (OD_{600} = 0.5). Chloramphenicol was added at a final concentration of 130 µg/mL and the culture was incubated for an additional 15 min at 37 °C (200 rpm). Next, the culture was split in 5 mL cultures and the test antibiotics were added at a final concentration of 10 x MIC. The cultures were incubated at 37 °C (200 rpm) for 1 h after which they were centrifuged for 5 min at 4 °C to pellet the bacteria (3,900 rpm). The supernatant was removed and the pellets were resuspended in 1 mL H_2O. The cells were lysed by boiling in a water bath at 100 °C for 15 min and subsequently centrifuged for 30 min (12,000 rpm). The supernatant of the samples was lyophilized and redissolved in 250 µL buffer A (50 mM ammonium bicarbonate, 5 mM NEt_3, pH 8.3). Samples were analyzed by analytical RP-HPLC at 214 nm using a 0-25% buffer B (MeOH) gradient over 25 min. The HPLC analysis was done using a Phenomenex Jupiter su C_{18} 300 Å column (250 x 4.60 mm, 5 µm) on a Shimadzu LC-2030 Plus instrument.

Hemolysis assays. Defibrinated whole sheep blood was centrifuged for 15 minutes at 4 °C (400 g). The top layer was discarded and the bottom layer was washed with phosphate buffered saline (PBS) and centrifuged for 15 min at 4 °C (400 g). Washing cycles were repeated at least three times. In polypropylene 96-well microtiter plates, 10-fold serial dilutions of antibiotics in PBS with 0.002% p80 in biological triplicates were added (75 µL) and an equal volume of packed blood cells diluted 25-fold in PBS with 0.002% p80 (75 µL) was added to all wells. The plates were incubated for 20 h at 37 °C with continuous shaking (500 rpm). After incubation, the plates were centrifuged for 5 min (800 g) and 25 µL of supernatant was transferred to a clear UV-star flat-bottom polystyrene 96-well plate already containing 100 µL H_2O per well. Absorption was measured at 415 nm. Data were corrected by subtraction of the background response of 1% DMSO in the presence of cells with no antibiotic and normalized using the absorbance of 0.1% Triton X-100 with blood cells as 100% hemolysis control.

5.5 Supplementary Information

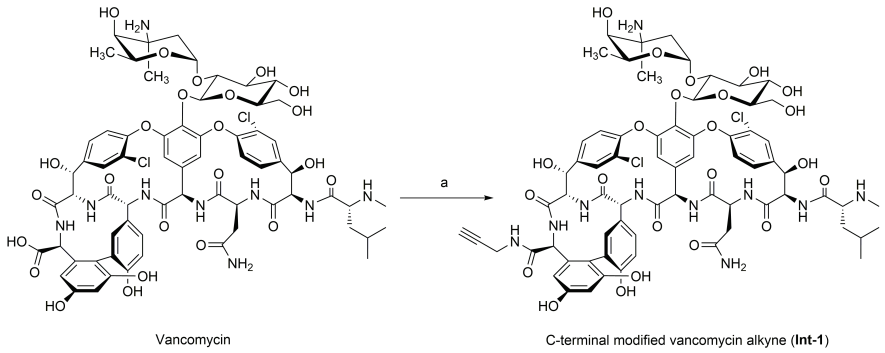

Scheme S1. The synthesis of Int-1. a) propargylamine, HBTU, DIPEA, DMF/DMSO, RT.

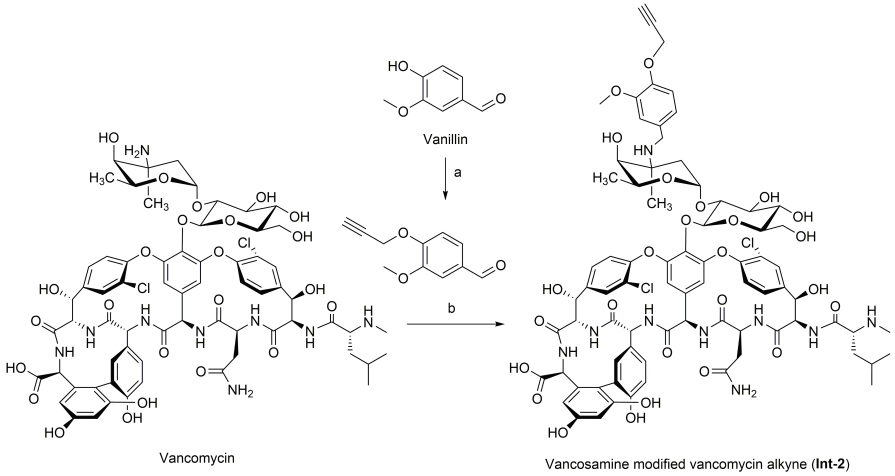

Scheme S2. The synthesis of Int-2. a) propargylbromide, K_2CO_3, DMF, RT; b) $NaBH_3CN$, DIPEA, DMF/MeOH, 70 °C then 50 °C.

Table S1. *In vitro* activity of the vancomycin-trihydroxamate sideromycins against a panel of Gram-negative strains in µM.

	MIC (µM)					
	E. coli			***K. pneumonia***	***A. baumannii***	***P. aeruginosa***
	ATCC 25992	**ATCC 35218**	**BW 25113**	**ATCC 13883**	**BAA-747**	**ATCC 27853**
Iron-repleted CAMHB						
Vancomycin	>86	>86	172	>86	>86	>86
1	>58	>58	>117	>58	>58	>58
2	>55	>55	>110	>55	>55	>55
12	>182	>182	>364	>182	>182	>182
Int-1	86	43	43	>86	>86	>86
Int-2	>79	>79	>158	>79	>79	>79
Iron-depleted CAMHB						
Vancomycin	>86	>86	86	>86	>86	>86
1	>58	>58	>117	>58	>58	>58
2	>55	>55	>110	>55	>55	>55
12	>182	>182	>364	>182	>182	>182
Int-1	43	43	43	>86	>86	>86
Int-2	>79	>79	>158	>79	>79	>79

5

Table S2. *In vitro* activity of the vancomycin-trihydroxamate sideromycins against *E. coli* BW25113 and *Δent* in µM with and without exogenous enterobactin supplementation.

	MIC (µM)		
	***E. coli* BW25113**		
	WT	***ΔentA***	***ΔentA* + 8 µg/mL enterobactin**
Iron-repleted CAMHB			
Vancomycin	172	86	86
1	>117	7	>117
2	>110	7	>110
12	>364	>364	>364
Int-1	43	43	43
Int-2	>158	>158	>158
Iron-depleted CAMHB			
Vancomycin	86	86	86
1	>117	4	>117
2	>110	3	>110
12	>364	>364	>364
Int-1	43	43	43
Int-2	>158	>158	>158

Table S3. *In vitro* activity of the vancomycin-trihydroxamate sideromycins against *E. coli* BW25113 and enterobactin biosynthesis, export and import deletion strains in µM.

	MIC (µM)						
	E. coli BW25113						
	WT	***ΔentA***	***ΔentC***	***ΔtolC***	***ΔfepA***	***ΔfepB***	***ΔfepD***
		biosynthesis		**export**	**import**		
Iron-repleted CAMHB							
Vancomycin	172	86	86	172	43	86	86
1	>117	7	15	15	58	29	29
2	>110	7	14	14	>110	110	>110
12	>364	>364	>364	>364	>364	>364	>364
Int-1	43	43	43	43	86	43	43
Int-2	>158	>158	>158	>158	>158	>158	>158
Iron-depleted CAMHB							
Vancomycin	86	86	86	86	43	43	43
1	>117	4	7	7	58	15	29
2	>110	3	7	7	>110	110	>110
12	>364	>364	>364	>364	>364	>364	>364
Int-1	43	43	43	43	43	43	43
Int-2	>158	>158	>158	>158	>158	>158	>158

5

Table S4. *In vitro* activity of the vancomycin-trihydroxamate sideromycins against *E. coli* BW25113 and *ΔentA* in µM in the presence and absence of exogenous outer membrane disruptor PMBN.

	MIC (µM)			
	E. coli BW25113			
	WT	**WT + 8 µg/mL PMBN**	***ΔentA***	***ΔentA* + 8 µg/mL PMBN**
Iron-repleted CAMHB				
Vancomycin	172	43	86	43
1	>117	29	7	7
2	>110	110	7	7
12	>364	>364	>364	>364
Int-1	43	22	43	22
Int-2	>158	79	>158	79
Iron-depleted CAMHB				
Vancomycin	86	43	86	22
1	>117	15	4	4
2	>110	55	3	3
12	>364	>364	>364	>364
Int-1	43	22	43	11
Int-2	>158	79	>158	39

Table S5. *In vitro* activity of the vancomycin-trihydroxamate sideromycins against Gram-positive *S. aureus* strains in µM.

	MIC (µM)			
	S. aureus			
	ATCC 29213	**MRSA USA300**	**NRS384**	**BR-VRSA**
Iron-repleted CAMHB				
Vancomycin	0.673	0.673	0.673	>86
1	4	4	4	>58
2	7	7	7	>55
12	>182	>182	>182	>182
Int-1	0.336	0.673	0.336	>86
Int-2	0.616	1	0.616	>79
Iron-depleted CAMHB				
Vancomycin	0.673	0.673	0.673	>86
1	2	4	4	>58
2	3	7	7	>55
12	>182	>182	>182	>182
Int-1	0.673	0.673	0.336	>86
Int-2	0.616	1	0.616	>79

Compound 1 (95.8% purity)

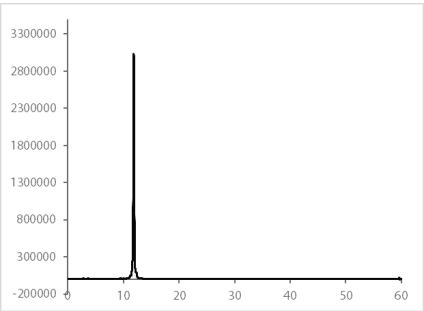

Compound 2 (97.5% purity)

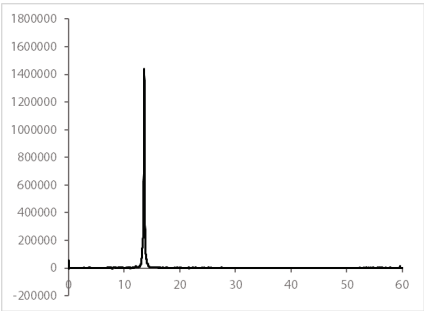

Compound 11(84.5% purity)

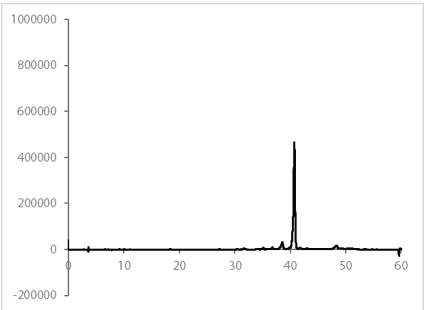

Compound 12 (95.0% purity for bioassays)

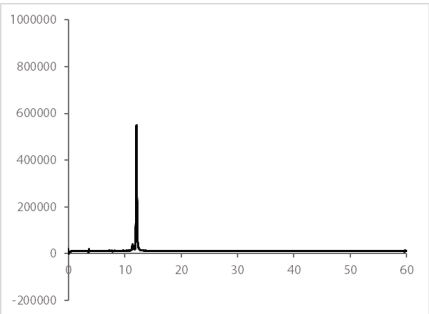

Fig. S1. Purity of final vancomycin-trihydroxamate sideromycins determined by analytical HPLC.

References

1. Murray, C. J. L., *et al.* Global burden of bacterial antimicrobial resistance in 2019: a systematic analysis. *Lancet* **399**, 629–655 (2022).
2. Rice, L. B. Federal Funding for the Study of Antimicrobial Resistance in Nosocomial Pathogens: No ESKAPE. *J. Infect. Dis.* **197**, 1079–1081 (2008).
3. Santajit, S. & Indrawattana, N. Mechanisms of Antimicrobial Resistance in ESKAPE Pathogens. *Biomed Res. Int.* **2016**, 2475067 (2016).
4. WHO. WHO publishes list of bacteria for which new antibiotics are urgently needed. https://www.who.int/news/item/27-02-2017-who-publishes-list-of-bacteria-for-which-new-antibiotics-are-urgently-needed (2017).
5. van Groesen, E., Slingerland, C. J., Innocenti, P., Mihajlovic, M., Masereeuw, R. & Martin, N. I. Vancomyxins: Vancomycin-Polymyxin Nonapeptide Conjugates That Retain Anti-Gram-Positive Activity with Enhanced Potency against Gram-Negative Strains. *ACS Infect. Dis.* **7**, 2746–2754 (2021).
6. Shi, W., Chen, F., Zou, X., Jiao, S., Wang, S., Hu, Y., Lan, L., Tang, F. & Huang, W. Design, synthesis, and antibacterial evaluation of vancomycin-LPS binding peptide conjugates. *Bioorg. Med. Chem. Lett.* **45**, 128122 (2021).
7. Antonoplis, A., Zang, X., Wegner, T., Wender, P. A. & Cegelski, L. Vancomycin-Arginine Conjugate Inhibits Growth of Carbapenem-Resistant E. coli and Targets Cell-Wall Synthesis. *ACS Chem. Biol.* **14**, 2065–2070 (2019).
8. Neville, L., Shalit, I., Warn, P. A., Scheetz, M. H., Sun, J., Chosy, M. B., Wender, P. A., Cegelski, L. & Rendell, J. T. In Vivo Targeting of Escherichia coli with Vancomycin-Arginine. *Antimicrob. Agents Chemother.* **65**, e02416-20 (2022).
9. Sarkar, P., Samaddar, S., Ammanathan, V., Yarlagadda, V., Ghosh, C., Shukla, M., Kaul, G., Manjithaya, R., Chopra, S. & Haldar, J. Vancomycin Derivative Inactivates Carbapenem-Resistant Acinetobacter baumannii and Induces Autophagy. *ACS Chem. Biol.* **15**, 884–889 (2020).
10. Guan, D., Chen, F., Qiu, Y., Jiang, B., Gong, L., Lan, L. & Huang, W. Sulfonium, an Underestimated Moiety for Structural Modification, Alters the Antibacterial Profile of Vancomycin Against Multidrug-Resistant Bacteria. *Angew. Chemie Int. Ed.* **58**, 6678–6682 (2019).
11. Ghosh, M. & Miller, M. J. Synthesis and in vitro antibacterial activity of spermidine-based mixed catechol- and hydroxamate-containing siderophore--vancomycin conjugates. *Bioorg. Med. Chem.* **4**, 43–48 (1996).
12. Levine, D. P. Vancomycin: A History. *Clin. Infect. Dis.* **42**, S5–S12 (2006).
13. Pootoolal, J., Neu, J. & Wright, G. D. Glycopeptide Antibiotic Resistance. *Annu. Rev. Pharmacol. Toxicol.* **42**, 381–408 (2002).
14. Walsh, C. T., Fisher, S. L., Park, I. S., Prahalad, M. & Wu, Z. Bacterial resistance to vancomycin: Five genes and one missing hydrogen bond tell the story. *Chem. Biol.* **3**, 21–28 (1996).
15. Blaskovich, M. A. T., Hansford, K. A., Butler, M. S., Jia, Z., Mark, A. E. & Cooper, M. A. Developments in Glycopeptide Antibiotics. *ACS Infect. Dis.* **4**, 715–735 (2018).
16. Barna, J. C. & Williams, D. H. The structure and mode of action of glycopeptide antibiotics of the vancomycin group. *Annu. Rev. Microbiol.* **38**, 339–357 (1984).
17. Williams, D. H. & Kalman, J. R. Structural and mode of action studies on the antibiotic vancomycin. Evidence from 270-MHz proton magnetic resonance. *J. Am. Chem. Soc.* **99**, 2768–2774 (1977).
18. Henderson, J. C., Zimmerman, S. M., Crofts, A. A., Boll, J. M., Kuhns, L. G., Herrera, C. M. & Trent, M. S. The Power of Asymmetry: Architecture and Assembly of the Gram-Negative Outer Membrane Lipid Bilayer. *Annu. Rev. Microbiol.* **70**, 255–278 (2016).
19. Shlaes, D. M., Shlaes, J. H., Davies, J. & Williamson, R. Escherichia coli susceptible to glycopeptide antibiotics. *Antimicrob. Agents Chemother.* **33**, 192–197 (1989).
20. Heesterbeek, D. A. C., Martin, N. I., Velthuizen, A., Duijst, M., Ruyken, M., Wubbolts, R., Rooijakkers, S. H. M. & Bardoel, B. W. Complement-dependent outer membrane perturbation sensitizes Gram-negative bacteria to Gram-positive specific antibiotics. *Sci. Rep.* **9**, 3074 (2019).
21. Stokes, J. M., MacNair, C. R., Ilyas, B., French, S., Côté, J.-P., Bouwman, C., Farha, M. A., Sieron, A. O., Whitfield, C., Coombes, B. K. & Brown, E. D. Pentamidine sensitizes Gram-negative pathogens to antibiotics and overcomes acquired colistin resistance. *Nat. Microbiol.* **2**, (2017).
22. Wesseling, C. M. J., Slingerland, C. J., Veraar, S., Lok, S. & Martin, N. I. Structure–Activity

Studies with Bis-Amidines That Potentiate Gram-Positive Specific Antibiotics against Gram-Negative Pathogens. *ACS Infect. Dis.* **7**, 3314–3335 (2021).
23. Li, Q., Cebrián, R., Montalbán-López, M., Ren, H., Wu, W. & Kuipers, O. P. Outer-membrane-acting peptides and lipid II-targeting antibiotics cooperatively kill Gram-negative pathogens. *Commun. Biol.* **4**, (2021).
24. Vaara, M. Agents that increase the permeability of the outer membrane. *Microbiol. Rev.* **56**, 395–411 (1992).
25. Ofek, I., Cohen, S., Rahmani, R., Kabha, K., Tamarkin, D., Herzig, Y. & Rubinstein, E. Antibacterial synergism of polymyxin B nonapeptide and hydrophobic antibiotics in experimental gram-negative infections in mice. *Antimicrob. Agents Chemother.* **38**, 374–377 (1994).
26. Ghosh, M., Miller, P. A. & Miller, M. J. Antibiotic repurposing: bis-catechol- and mixed ligand (bis-catechol-mono-hydroxamate)-teicoplanin conjugates are active against multidrug resistant Acinetobacter baumannii. *J. Antibiot.* **73**, 152–157 (2020).
27. Zheng, T., Bullock, J. L. & Nolan, E. M. Siderophore-Mediated Cargo Delivery to the Cytoplasm of Escherichia coli and Pseudomonas aeruginosa: Syntheses of Monofunctionalized Enterobactin Scaffolds and Evaluation of Enterobactin–Cargo Conjugate Uptake. *J. Am. Chem. Soc.* **134**, 18388–18400 (2012).
28. Kramer, J., Özkaya, Ö. & Kümmerli, R. Bacterial siderophores in community and host interactions. *Nat. Rev. Microbiol.* **18**, 152–163 (2020).
29. Byers, B. R. & Arceneaux, J. E. Microbial iron transport: iron acquisition by pathogenic microorganisms. *Met. Ions Biol. Syst.* **35**, 37–66 (1998).
30. Andrews, S. C., Robinson, A. K. & Rodríguez-Quiñones, F. Bacterial iron homeostasis. *FEMS Microbiol. Rev.* **27**, 215–237 (2003).
31. Hider, R. C. & Kong, X. Chemistry and biology of siderophores. *Nat. Prod. Rep.* **27**, 637–657 (2010).
32. Goswami, M., Subramanian, M., Kumar, R., Jass, J. & Jawali, N. Involvement of Antibiotic Efflux Machinery in Glutathione-Mediated Decreased Ciprofloxacin Activity in Escherichia coli. *Antimicrob. Agents Chemother.* **60**, 4369–4374 (2016).
33. Sato, T. & Yamawaki, K. Cefiderocol: Discovery, Chemistry, and In Vivo Profiles of a Novel Siderophore Cephalosporin. *Clin. Infect. Dis.* **69**, S538–S543 (2019).
34. Miethke, M. & Marahiel, M. A. Siderophore-based iron acquisition and pathogen control. *Microbiol. Mol. Biol. Rev.* **71**, 413–451 (2007).
35. Harris, W. R., Carrano, C. J., Cooper, S. R., Sofen, S. R., Avdeef, A. E., McArdle, J. V & Raymond, K. N. Coordination chemistry of microbial iron transport compounds. 19. Stability constants and electrochemical behavior of ferric enterobactin and model complexes. *J. Am. Chem. Soc.* **101**, 6097–6104 (1979).
36. Marlovits, T. C., Haase, W., Herrmann, C., Aller, S. G. & Unger, V. M. The membrane protein FeoB contains an intramolecular G protein essential for Fe(II) uptake in bacteria. *Proc. Natl. Acad. Sci.* **99**, 16243–16248 (2002).
37. Genco, C. A. & Dixon, D. W. Emerging strategies in microbial haem capture. *Mol. Microbiol.* **39**, 1–11 (2001).
38. Wandersman, C. & Delepelaire, P. Bacterial iron sources: from siderophores to hemophores. *Annu. Rev. Microbiol.* **58**, 611–647 (2004).
39. Raymond, K. N., Dertz, E. A. & Kim, S. S. Enterobactin: An archetype for microbial iron transport. *Proc. Natl. Acad. Sci.* **100**, 3584–3588 (2003).
40. Saha, M., Sarkar, S., Sarkar, B., Sharma, B. K., Bhattacharjee, S. & Tribedi, P. Microbial siderophores and their potential applications: a review. *Environ. Sci. Pollut. Res.* **23**, 3984–3999 (2016).
41. Kell, D. B., Heyden, E. L. & Pretorius, E. The Biology of Lactoferrin, an Iron-Binding Protein That Can Help Defend Against Viruses and Bacteria. *Front. Immunol.* **11**, (2020).
42. Page, M. G. P. The Role of Iron and Siderophores in Infection, and the Development of Siderophore Antibiotics. *Clin. Infect. Dis.* **69**, S529–S537 (2019).
43. Sriyosachati, S. & Cox, C. D. Siderophore-mediated iron acquisition from transferrin by Pseudomonas aeruginosa. *Infect. Immun.* **52**, 885–891 (1986).
44. Faraldo-Gómez, J. D. & Sansom, M. S. P. Acquisition of siderophores in Gram-negative bacteria. *Nat. Rev. Mol. Cell Biol.* **4**, 105–116 (2003).
45. Chu, B. C., Garcia-Herrero, A., Johanson, T. H., Krewulak, K. D., Lau, C. K., Peacock, R. S., Slavinskaya, Z. & Vogel, H. J. Siderophore uptake in bacteria and the battle for iron with the host; a

bird's eye view. *Biometals* **23**, 601–611 (2010).
46. Hassan, H. & Troxell, B. Transcriptional regulation by Ferric Uptake Regulator (Fur) in pathogenic bacteria. *Front. Cell. Infect. Microbiol.* **3**, (2013).
47. Escolar, L., Pérez-Martín, J. & de Lorenzo, V. Opening the Iron Box: Transcriptional Metalloregulation by the Fur Protein. *J. Bacteriol.* **181**, 6223–6229 (1999).
48. Lamont, I. L., Beare, P. A., Ochsner, U., Vasil, A. I. & Vasil, M. L. Siderophore-mediated signaling regulates virulence factor production in Pseudomonas aeruginosa. *Proc. Natl. Acad. Sci.* **99**, 7072–7077 (2002).
49. Braun, V., Pramanik, A., Gwinner, T., Köberle, M. & Bohn, E. Sideromycins: tools and antibiotics. *Biometals* **22**, 3–13 (2009).
50. Reynolds, D. M., Schatz, A. & Waksman, S. A. Grisein, a New Antibiotic Produced by a Strain of Streptomyces griseus. *Proc. Soc. Exp. Biol. Med.* **64**, 50–54 (1947).
51. Stapley, E. O. & Ormond, R. E. Similarity of Albomycin and Grisein. *Science* **125**, 587–589 (1957).
52. Lin, Z., Xu, X., Zhao, S., Yang, X., Guo, J., Zhang, Q., Jing, C., Chen, S. & He, Y. Total synthesis and antimicrobial evaluation of natural albomycins against clinical pathogens. *Nat. Commun.* **9**, (2018).
53. Gause, G. F. Recent studies on albomycin, a new antibiotic. *Br. Med. J.* **2**, 1177–1179 (1955).
54. Benz, G., Schröder, T., Kurz, J., Wünsche, C., Karl, W., Steffens, G., Pfitzner, J. & Schmidt, D. Konstitution der Desferriform der Albomycine δ1, δ2, ε. *Angew. Chemie* **21**, 1322–1335 (1982).
55. Ferguson, A. D., Braun, V., Fiedler, H. P., Coulton, J. W., Diederichs, K. & Welte, W. Crystal structure of the antibiotic albomycin in complex with the outer membrane transporter FhuA. *Protein Sci.* **9**, 956–963 (2000).
56. Locher, K. P., Rees, B., Koebnik, R., Mitschler, A., Moulinier, L., Rosenbusch, J. P. & Moras, D. Transmembrane signaling across the ligand-gated FhuA receptor: crystal structures of free and ferrichrome-bound states reveal allosteric changes. *Cell* **95**, 771–778 (1998).
57. Braun, V. Active transport of siderophore-mimicking antibacterials across the outer membrane. *Drug Resist. Updat.* **2**, 363–369 (1999).
58. Moeck, G. S., Coulton, J. W. & Postle, K. Cell envelope signaling in Escherichia coli. Ligand binding to the ferrichrome-iron receptor fhua promotes interaction with the energy-transducing protein TonB. *J. Biol. Chem.* **272**, 28391–28397 (1997).
59. Braun, V. Energy-coupled transport and signal transduction through the gram-negative outer membrane via TonB-ExbB-ExbD-dependent receptor proteins. *FEMS Microbiol. Rev.* **16**, 295–307 (1995).
60. Günter, K. & Braun, V. In vivo evidence for FhuA outer membrane receptor interaction with the TonB inner membrane protein of Escherichia coli. *FEBS Lett.* **274**, 85–88 (1990).
61. Köster, W. & Braun, V. Iron (III) hydroxamate transport into Escherichia coli. Substrate binding to the periplasmic FhuD protein. *J. Biol. Chem.* **265**, 21407–21410 (1990).
62. Köster, W. & Braun, V. Iron-hydroxamate transport into Escherichia coli K12: Localization of FhuD in the periplasm and of FhuB in the cytoplasmic membrane. *Mol. Gen. Genet. MGG* **217**, 233–239 (1989).
63. Burkhardt, R. & Braun, V. Nucleotide sequence of the fhuC and fhuD genes involved in iron (III) hydroxamate transport: Domains in FhuC homologous to ATP-binding proteins. *Mol. Gen. Genet. MGG* **209**, 49–55 (1987).
64. Schultz-Hauser, G., Köster, W., Schwarz, H. & Braun, V. Iron(III) hydroxamate transport in Escherichia coli K-12: FhuB-mediated membrane association of the FhuC protein and negative complementation of fhuC mutants. *J. Bacteriol.* **174**, 2305–2311 (1992).
65. Köster, W. & Braun, V. Iron hydroxamate transport of Escherichia coli: nucleotide sequence of the fhuB gene and identification of the protein. *Mol. Gen. Genet.* **204**, 435–442 (1986).
66. Braun, V., Günthner, K., Hantke, K. & Zimmermann, L. Intracellular activation of albomycin in Escherichia coli and Salmonella typhimurium. *J. Bacteriol.* **156**, 308–315 (1983).
67. Hartmann, A., Fiedler, H. P. & Braun, V. Uptake and conversion of the antibiotic albomycin by Escherichia coli K-12. *Eur. J. Biochem.* **99**, 517–524 (1979).
68. Pramanik, A., Stroeher, U. H., Krejci, J., Standish, A. J., Bohn, E., Paton, J. C., Autenrieth, I. B. & Braun, V. Albomycin is an effective antibiotic, as exemplified with Yersinia enterocolitica and Streptococcus pneumoniae. *Int. J. Med. Microbiol.* **297**, 459–469 (2007).
69. Pramanik, A. & Braun, V. Albomycin Uptake via a Ferric Hydroxamate Transport System of *Streptococcus pneumoniae* R6. *J. Bacteriol.* **188**, 3878–3886 (2006).
70. Zähner, H., Diddens, H., Keller-Schierlein, W. & Nägeli, H. U. Some experiments with

semisynthetic sideromycins. *Jpn. J. Antibiot.* **30 Suppl**, 201–206 (1977).
71. Ghosh, M., Miller, P. A., Möllmann, U., Claypool, W. D., Schroeder, V. A., Wolter, W. R., Suckow, M., Yu, H., Li, S., Huang, W., Zajicek, J. & Miller, M. J. Targeted Antibiotic Delivery: Selective Siderophore Conjugation with Daptomycin Confers Potent Activity against Multidrug Resistant Acinetobacter baumannii Both in Vitro and in Vivo. *J. Med. Chem.* **60**, 4577–4583 (2017).
72. Pinkert, L., Lai, Y.-H., Peukert, C., Hotop, S.-K., Karge, B., Schulze, L. M., Grunenberg, J. & Brönstrup, M. Antibiotic Conjugates with an Artificial MECAM-Based Siderophore Are Potent Agents against Gram-Positive and Gram-Negative Bacterial Pathogens. *J. Med. Chem.* **64**, 15440–15460 (2021).
73. Wencewicz, T. A. & Miller, M. J. Biscatecholate–Monohydroxamate Mixed Ligand Siderophore–Carbacephalosporin Conjugates are Selective Sideromycin Antibiotics that Target Acinetobacter baumannii. *J. Med. Chem.* **56**, 4044–4052 (2013).
74. Liu, R., Miller, P. A., Vakulenko, S. B., Stewart, N. K., Boggess, W. C. & Miller, M. J. A Synthetic Dual Drug Sideromycin Induces Gram-Negative Bacteria To Commit Suicide with a Gram-Positive Antibiotic. *J. Med. Chem.* **61**, 3845–3854 (2018).
75. Negash, K. H., Norris, J. K. S. & Hodgkinson, J. T. Siderophore-Antibiotic Conjugate Design: New Drugs for Bad Bugs? *Molecules* **24**, 3314 (2019).
76. Zhanel, G. G., Golden, A. R., Zelenitsky, S., Wiebe, K., Lawrence, C. K., Adam, H. J., Idowu, T., Domalaon, R., Schweizer, F., Zhanel, M. A., Lagacé-Wiens, P. R. S., Walkty, A. J., Noreddin, A., Lynch III, J. P. & Karlowsky, J. A. Cefiderocol: A Siderophore Cephalosporin with Activity Against Carbapenem-Resistant and Multidrug-Resistant Gram-Negative Bacilli. *Drugs* **79**, 271–289 (2019).
77. Ohi, N., Aoki, B., Shinozaki, T., Moro, K., Noto, T., Nehashi, T., Okazaki, H. & Matsunaga, I. Semisynthetic beta-lactam antibiotics. I. Synthesis and antibacterial activity of new ureidopenicillin derivatives having catechol moieties. *J. Antibiot.* **39**, 230–241 (1986).
78. Dolence, E. K., Lin, C. E., Miller, M. J. & Payne, S. M. Synthesis and siderophore activity of albomycin-like peptides derived from N5-acetyl-N5-hydroxy-L-ornithine. *J. Med. Chem.* **34**, 956–968 (1991).
79. Lin, Y.-M., Ghosh, M., Miller, P. A., Möllmann, U. & Miller, M. J. Synthetic sideromycins (skepticism and optimism): selective generation of either broad or narrow spectrum Gram-negative antibiotics. *Biometals* **32**, 425–451 (2019).
80. Ghosh, M., Lin, Y.-M., Miller, P. A., Möllmann, U., Boggess, W. C. & Miller, M. J. Siderophore Conjugates of Daptomycin are Potent Inhibitors of Carbapenem Resistant Strains of Acinetobacter baumannii. *ACS Infect. Dis.* **4**, 1529–1535 (2018).
81. Brochu, A., Brochu, N., Nicas, T. I., Parr, T. R. J., Minnick, A. A. J., Dolence, E. K., McKee, J. A., Miller, M. J., Lavoie, M. C. & Malouin, F. Modes of action and inhibitory activities of new siderophore-beta-lactam conjugates that use specific iron uptake pathways for entry into bacteria. *Antimicrob. Agents Chemother.* **36**, 2166–2175 (1992).
82. Shionogi. Shionogi Announces FDA Approval of FETROJA® (Cefiderocol) for the Treatment of Hospital-Acquired Bacterial Pneumonia and Ventilator-Associated Bacterial Pneumonia. https://www.shionogi.com/us/en/news/2020/9/shionogi-announces-fda-approval-of-fetroja-cefiderocol-for-the-treatment-of-hospital-acquired-bacterial-pneumonia-and-ventilator-associated-bacterial-pneumonia.html (2020).
83. Paulen, A., Gasser, V., Hoegy, F., Perraud, Q., Pesset, B., Schalk, I. J. & Mislin, G. L. A. Synthesis and antibiotic activity of oxazolidinone-catechol conjugates against Pseudomonas aeruginosa. *Org. Biomol. Chem.* **13**, 11567–11579 (2015).
84. Ghosh, M. & Miller, M. J. Design, synthesis, and biological evaluation of isocyanurate-based antifungal and macrolide antibiotic conjugates: iron transport-mediated drug delivery. *Bioorg. Med. Chem.* **3**, 1519–1525 (1995).
85. Zheng, T. & Nolan, E. M. Enterobactin-Mediated Delivery of β-Lactam Antibiotics Enhances Antibacterial Activity against Pathogenic Escherichia coli. *J. Am. Chem. Soc.* **136**, 9677–9691 (2014).
86. Rostovtsev, V. V, Green, L. G., Fokin, V. V & Sharpless, K. B. A Stepwise Huisgen Cycloaddition Process: Copper(I)-Catalyzed Regioselective "Ligation" of Azides and Terminal Alkynes. *Angew. Chemie Int. Ed.* **41**, 2596–2599 (2002).
87. Tornøe, C. W., Christensen, C. & Meldal, M. Peptidotriazoles on Solid Phase: [1,2,3]-Triazoles by Regiospecific Copper(I)-Catalyzed 1,3-Dipolar Cycloadditions of Terminal Alkynes to Azides. *J. Org. Chem.* **67**, 3057–3064 (2002).

88. Silverman, S. M., Moses, J. E. & Sharpless, K. B. Reengineering Antibiotics to Combat Bacterial Resistance: Click Chemistry [1,2,3]-Triazole Vancomycin Dimers with Potent Activity against MRSA and VRE. *Chem. – A Eur. J.* **23**, 79–83 (2017).
89. Blaskovich, M. A. T., Hansford, K. A., Butler, M. S., Jia, Z., Mark, A. E. & Cooper, M. A. Developments in Glycopeptide Antibiotics. *ACS Infect. Dis.* **4**, 715–735 (2018).
90. Hanna, J. R., Allan, C., Lawrence, C., Meyer, O., Wilson, N. D. & Hulme, A. N. Optimizing the Readout of Lanthanide-DOTA Complexes for the Detection of Ligand-Bound Copper(I). *Molecules* **22**, 802 (2017).
91. Benz, G. & Schmidt, D. Albomycine, IV. Isolierung und Totalsynthese von (N5-Acetyl-N5-hydroxy-L-ornithyl)-(N5-acetyl-N5-hydroxy-L-ornithyl)-N5-acetyl-N5-hydroxy-L-ornithin. *European J. Org. Chem.* **1984**, 1434–1440 (1984).
92. Olsen, R. K., Ramasamy, K. & Emery, T. Synthesis of Nα,Nδ-Protected Nδ-Hydroxy-L-ornithine from L-Glutamic Acid. *J. Org. Chem.* **49**, 3527–3534 (1984).
93. Lin, Y.-M. & Miller, M. J. Practical Synthesis of Hydroxamate-Derived Siderophore Components by an Indirect Oxidation Method and Syntheses of a DIG−Siderophore Conjugate and a Biotin−Siderophore Conjugate. *J. Org. Chem.* **64**, 7451–7458 (1999).
94. Dolence, E. K., Minnick, A. A. & Miller, M. J. N5-Acetyl-N5-hydroxy-L-ornithine-derived siderophore-carbacephalosporin .beta.-lactam conjugates: iron transport mediated drug delivery. *J. Med. Chem.* **33**, 461–464 (1990).
95. Katritzky, A. R., Angrish, P., Hür, D. & Suzuki, K. N-(Cbz- and Fmoc-α-aminoacyl)benzotriazoles: Stable Derivatives Enabling Peptide Coupling of Tyr, Trp, Cys, Met, and Gln with Free Amino Acids in Aqueous Media with Complete Retention of Chirality. *Synthesis* **2005**, 397–402 (2005).
96. Katritzky, A. R., Yoshioka, M., Narindoshvili, T., Chung, A. & Khashab, N. M. N-Fmoc-Protected(α-Dipeptidoyl)Benzotriazoles for Efficient Solid-Phase Peptide Synthesis by Segment Condensation. *Chem. Biol. Drug Des.* **72**, 182–188 (2008).
97. Katritzky, A. R., Haase, D. N., Johnson, J. V & Chung, A. Benzotriazole-Assisted Solid-Phase Assembly of Leu-Enkephalin, Amyloid β segment 34−42, and other "Difficult" Peptide Sequences. *J. Org. Chem.* **74**, 2028–2032 (2009).
98. Katritzky, A. R., Todadze, E., Shestopalov, A. A., Cusido, J. & Angrish, P. Selective Peptide Chain Extension at the C-terminus of Aspartic and Glutamic Acids Utilizing N-protected (α-aminoacyl)benzotriazoles. *Chem. Biol. Drug Des.* **68**, 42–47 (2006).
99. Chan, T. R., Hilgraf, R., Sharpless, K. B. & Fokin, V. V. Polytriazoles as Copper(I)-Stabilizing Ligands in Catalysis. *Org. Lett.* **6**, 2853–2855 (2004).
100. Gotsbacher, M. P. & Codd, R. Azido-Desferrioxamine Siderophores as Functional Click-Chemistry Probes Generated in Culture upon Adding a Diazo-Transfer Reagent. *Chembiochem* **21**, 1433–1445 (2020).
101. Schalk, I. J., Mislin, G. L. A. & Brillet, K. Chapter Two - Structure, Function and Binding Selectivity and Stereoselectivity of Siderophore–Iron Outer Membrane Transporters. in *Current Topics in Membranes - Metal Transporters* (eds. Argüello, J. M. & Lutsenko, S. B. T.) vol. 69 37–66 (Academic Press, 2012).
102. Ito, A., Kohira, N., Bouchillon, S. K., West, J., Rittenhouse, S., Sader, H. S., Rhomberg, P. R., Jones, R. N., Yoshizawa, H., Nakamura, R., Tsuji, M. & Yamano, Y. In vitro antimicrobial activity of S-649266, a catechol-substituted siderophore cephalosporin, when tested against non-fermenting Gram-negative bacteria. *J. Antimicrob. Chemother.* **71**, 670–677 (2015).
103. Kohira, N., West, J., Ito, A., Ito-Horiyama, T., Nakamura, R., Sato, T., Rittenhouse, S., Tsuji, M. & Yamano, Y. *In Vitro* Antimicrobial Activity of a Siderophore Cephalosporin, S-649266, against Enterobacteriaceae Clinical Isolates, Including Carbapenem-Resistant Strains. *Antimicrob. Agents Chemother.* **60**, 729–734 (2016).
104. Hackel, M. A., Tsuji, M., Yamano, Y., Echols, R., Karlowsky, J. A. & Sahm, D. F. Reproducibility of broth microdilution MICs for the novel siderophore cephalosporin, cefiderocol, determined using iron-depleted cation-adjusted Mueller-Hinton broth. *Diagn. Microbiol. Infect. Dis.* **94**, 321–325 (2019).
105. Ito, A., Nishikawa, T., Matsumoto, S., Yoshizawa, H., Sato, T., Nakamura, R., Tsuji, M. & Yamano, Y. Siderophore Cephalosporin Cefiderocol Utilizes Ferric Iron Transporter Systems for Antibacterial Activity against Pseudomonas aeruginosa. *Antimicrob. Agents Chemother.* **60**, 7396–7401 (2016).
106. Cornelis, P., Hohnadel, D. & Meyer, J. M. Evidence for different pyoverdine-mediated iron uptake systems among Pseudomonas aeruginosa strains. *Infect. Immun.* **57**, 3491–3497 (1989).

107. Meyer, J. M. Pyoverdines: pigments, siderophores and potential taxonomic markers of fluorescent Pseudomonas species. *Arch. Microbiol.* **174**, 135–142 (2000).
108. Tomaras, A. P., Crandon, J. L., McPherson, C. J., Banevicius, M. A., Finegan, S. M., Irvine, R. L., Brown, M. F., O'Donnell, J. P. & Nicolau, D. P. Adaptation-based resistance to siderophore-conjugated antibacterial agents by Pseudomonas aeruginosa. *Antimicrob. Agents Chemother.* **57**, 4197–4207 (2013).
109. Minnick, A. A., McKee, J. A., Dolence, E. K. & Miller, M. J. Iron transport-mediated antibacterial activity of and development of resistance to hydroxamate and catechol siderophore-carbacephalosporin conjugates. *Antimicrob. Agents Chemother.* **36**, 840–850 (1992).
110. Grenier, F., Matteau, D., Baby, V. & Rodrigue, S. Complete Genome Sequence of Escherichia coli BW25113. *Genome Announc.* **2**, e01038-14 (2014).
111. Baba, T., Ara, T., Hasegawa, M., Takai, Y., Okumura, Y., Baba, M., Datsenko, K. A., Tomita, M., Wanner, B. L. & Mori, H. Construction of Escherichia coli K-12 in-frame, single-gene knockout mutants: the Keio collection. *Mol. Syst. Biol.* **2**, (2006).
112. Liu, J., Duncan, K. & Walsh, C. T. Nucleotide sequence of a cluster of Escherichia coli enterobactin biosynthesis genes: identification of entA and purification of its product 2,3-dihydro-2,3-dihydroxybenzoate dehydrogenase. *J. Bacteriol.* **171**, 791–798 (1989).
113. Walsh, C. T., Liu, J., Rusnak, F. & Sakaitani, M. Molecular studies on enzymes in chorismate metabolism and the enterobactin biosynthetic pathway. *Chem. Rev.* **90**, 1105–1129 (1990).
114. Vega, D. E. & Young, K. D. Accumulation of periplasmic enterobactin impairs the growth and morphology of Escherichia coli tolC mutants. *Mol. Microbiol.* **91**, 508–521 (2014).
115. Ozenberger, B. A., Nahlik, M. S. & McIntosh, M. A. Genetic organization of multiple fep genes encoding ferric enterobactin transport functions in Escherichia coli. *J. Bacteriol.* **169**, 3638–3646 (1987).
116. Pierce, J. R. & Earhart, C. F. Escherichia coli K-12 envelope proteins specifically required for ferrienterobactin uptake. *J. Bacteriol.* **166**, 930–936 (1986).
117. Chenault, S. S. & Earhart, C. F. Identification of hydrophobic proteins FepD and FepG of the Escherichia coli ferrienterobactin permease. *Microbiology* **138**, 2167–2171 (1992).
118. Fischbach, M. A., Lin, H., Liu, D. R. & Walsh, C. T. How pathogenic bacteria evade mammalian sabotage in the battle for iron. *Nat. Chem. Biol.* **2**, 132–138 (2006).
119. Casanova-Hampton, K., Carey, A., Kassam, S., Garner, A., Donati, G. L., Thangamani, S. & Subashchandrabose, S. A genome-wide screen reveals the involvement of enterobactin-mediated iron acquisition in Escherichia coli survival during copper stress. *Metallomics* **13**, (2021).
120. Orchard, S. S., Rostron, J. E. & Segall, A. M. Escherichia coli enterobactin synthesis and uptake mutants are hypersensitive to an antimicrobial peptide that limits the availability of iron in addition to blocking Holliday junction resolution. *Microbiology* **158**, 547–559 (2012).
121. Peralta, D. R., Adler, C., Corbalán, N. S., Paz García, E. C., Pomares, M. F. & Vincent, P. A. Enterobactin as Part of the Oxidative Stress Response Repertoire. *PLoS One* **11**, e0157799 (2016).
122. Vaara, M., Viljanen, P., Vaara, T. & Mäkelä, P. H. An outer membrane-disorganizing peptide PMBN sensitizes E. coli strains to serum bactericidal action. *J. Immunol.* **132**, 2582–2589 (1984).
123. Garčic, A. A highly sensitive, simple determination of serum iron using chromazurol B. *Clin. Chim. Acta* **94**, 115–119 (1979).
124. Himpsl, S. D. & Mobley, H. L. T. Siderophore Detection Using Chrome Azurol S and Cross-Feeding Assays. in *Proteus mirabilis: Methods and Protocols* (ed. Pearson, M. M.) 97–108 (Springer New York, 2019).
125. Reynolds, P. E. Studies on the mode of action of vancomycin. *Biochim. Biophys. Acta* **52**, 403–405 (1961).
126. Somner, E. A. & Reynolds, P. E. Inhibition of peptidoglycan biosynthesis by ramoplanin. *Antimicrob. Agents Chemother.* **34**, 413–419 (1990).
127. Siewert, G. & Strominger, J. L. Bacitracin: an inhibitor of the dephosphorylation of lipid pyrophosphate, an intermediate in the biosynthesis of the peptidoglycan of bacterial cell walls. *Proc. Natl. Acad. Sci.* **57**, 767–773 (1967).
128. Simner, P. J. & Patel, R. Cefiderocol Antimicrobial Susceptibility Testing Considerations: the Achilles' Heel of the Trojan Horse? *J. Clin. Microbiol.* **59**, e00951-20 (2020).
129. Proença, D. N., Heine, T., Senges, C. H. R., Bandow, J. E., Morais, P. V & Tischler, D. Bacterial Metabolites Produced Under Iron Limitation Kill Pinewood Nematode and Attract Caenorhabditis elegans. *Front. Microbiol.* **10**, (2019).